Influence of analgesia on inflammation and NF-κB response in the murine intestine

Master thesis
M. Sc. Pharmaceutical Biotechnology
Submitted by

Lisa Drees
Registration number: [redacted]

1st reviewer:
Prof. Dr. Julien Béthune (HAW Hamburg)

2nd reviewer:
Dr. Dr. Marina Kolesnichenko (Charité Berlin)

27.02.2025, Hamburg

Abstract

Inflammatory bowel diseases, including ulcerative colitis (UC), cause chronic inflammation of the colon and/or the small intestine. The dextran sulfate sodium (DSS) induced colitis model is widely used to study UC but raises ethical concerns due to symptoms like bloody diarrhea and abdominal cramps. Following the 3R principle, animal suffering must be minimized while ensuring the accuracy of research outcomes. Providing analgesia in this model is challenging, as many analgesics can interfere with inflammation, epithelial integrity, and immune responses, potentially compromising research outcomes. The aim of this study was to identify the most suitable analgesic for use in DSS induced UC research, with limited interference with intestinal inflammation and NF-κB activity.

To achieve this, a deep learning-based tool, PEDL+, was used to identify amantadine and piritramide as the most promising candidates, while tramadol and paracetamol were included as positive controls based on LAGeSo recommendations. In the healthy colon, all analgesics increased goblet cell size, suggesting a general effect on mucin production. Among them, amantadine-treated mice showed the most similar goblet cell number, goblet cell size, and NF-κB activity to untreated controls, making it the most promising candidate for minimizing interference in colitis studies. In contrast, tramadol significantly influenced epithelial cell proliferation and NF-κB activity, while paracetamol significantly affected macrophage numbers and goblet cell dynamics. This shows that commonly used analgesics can introduce significant biases in UC research, while it also validates the effectiveness of PEDL+, as the pre-selected drugs, amantadine and piritramide, performed better than tramadol and paracetamol.

In the DSS UC model, amantadine had protective effects on epithelial integrity, reduced T-cell numbers, and decreased NF-κB activity in the colon. While these effects suggest potential anti-inflammatory properties, they also indicate interference with key research targets in UC studies. A similar trend was observed in the small intestine, where amantadine treatment led to a reduction in T-cells and NF-κB activity, despite no major structural changes in the ileum. This shows that even the most promising candidate, amantadine, is not ideal for all research applications. While it may be suitable for certain studies, it does influence NF-κB activity and immune responses. From a 3R perspective, avoiding analgesics when possible, would allow collected biopsies to be used for a broader range of analyses, reducing the need for additional animal experiments. If analgesics are used, they should be carefully chosen based on the primary research targets.

Content

List of abbreviations

AI	artificial intelligence
BAFFR	B-cell activation factor receptor
BWI	backwash ileitis
°C	degree Celsius
CD	Crohn's disease
ddH_2O	double deionized water
DNA	desoxyribonucleic acid
DSS	dextran sulphate sodium
EDTA	Ethylenediaminetetraacetic acid
EGFP	enhanced green fluorescent protein
g	gram
H&E	Hematoxylin and Eosin
IBD	inflammatory bowel disease
IF	immunofluorescence
IKK	IκB kinase
IL	interleukin
l	liter
LAGeSo	Landesamt für Gesundheit und Soziales
MAdCAM-1	mucosal vascular addressing cell adhesion molecule 1
MDC	Max Delbrück Center
mg	milligram
MGS	mouse grimace scale
ml	milliliter
mM	milli molar
NEMO	NF-κB essential modulator
NIK	NF-κB inducing kinase
NKT	natural killer T-cell
NSAID	nonsteroidal anti-inflammatory drug
PBS	phosphate buffered saline
PCR	polymerase chain reaction
PEDL	PPA Extraction with Deep Language
PPA	protein-protein association

RANK	receptor activator for NF-κB
rpm	rotations per minute
SII	small intestine ileum
TAE	TRIS-acetate-EDTA buffer
TBST	Tris buffered saline with Tween®
Th	T-helper cell
TLR	toll-like receptor
Treg	regulatory T-cell
TNF	tumor necrosis factor
TNFR	TNF receptors
µg	microgram
µl	microliter
UC	ulcerative colitis

List of figures

List of tables

1. Introduction

1.1. Animal models in biomedical research

Animals have been used for centuries as a model for the study of human anatomy, physiology, pathology and pharmacology, and contributed significantly to many important findings.[1] Monkeys were used for the development of the polio vaccine and the better understanding of the progress of disease.[2] The transplantation of organs was first studied in animals, making it possible to now perform life-saving transplantations in humans.[3] Experiments in dogs led to the discovery of insulin in the 1920s, which paved the way for modern insulin therapy.[4] Overall, animal models have led to numerous great advancements in many biological research fields and almost 90 % of Nobel prize research in physiology and medicine is based on animal experiments.[5]

Today, the most used animal models are rodents, namely mice. In 2023 over a million of mice were used in scientific research in Germany alone, making up 73 % of all used animals in experiments.[6] Given the widespread use of mice in biomedical research, it is essential to consider the ethical implications of animal experimentation, which play an important role to ensure humane treatment of the animals and minimize harm.

1.1.1. The 3R principle

In 1956 the scientists W.M.S. Russel and R.L. Buch defined the 3R principles. They are the basis for animal welfare policies and practices of modern research approaches. The three R's stand for Replacement, Reduction, and Refinement.[7] Replacement stands for the substitution of living, sentient higher animals for insentient material or animals, such as *D. melanogaster*. Reduction means, that if animals are being used, the number of animals employed should be reduced to the necessary amount, while still obtaining the information needed at a set amount and precision. Refinement is the process of decreasing the severity or incidence of inhumane or painful procedures, for the animals that must be used.[8] There can of course be overlap between the different categories. For instance, using animal tissue cultures can be seen as a replacement, because it is a substitution of live animals for insentient material, but it is also a reduction, since a single animal can supply for multiple cell cultures. In addition, it is also a refinement, because the animal can be euthanized painlessly and humanely instead of undergoing a treatment while still being alive.[8,9] Those principles are being followed until today and are part of the EU guidelines for protection of animals used for scientific purposes.[10]

Despite efforts to follow the 3R principles, animal models remain indispensable for studying complex, multi-organ diseases, like inflammatory bowel diseases (IBD). Replacement encourages the use of in vitro methods, such as cell cultures or organoids, to avoid animal use. While these alternatives are cost-effective and can be generated quickly, they have significant limitations. For instance, the intricate environment of an organism cannot be exactly replicated, like the interaction of organs and the distinct cellular and molecular mechanisms along with microbiota composition. IBD, characterized by chronic inflammation of the gastrointestinal tract, is a prime example of a condition that often requires animal models to investigate its underlying mechanisms and potential treatments.[11,12]

1.2. Inflammatory bowel diseases

Inflammatory bowel diseases are characterized by chronic inflammation of the colon and sometimes the small intestine. The inflammation and ulceration of the intestinal mucosa is a result of the infiltration of neutrophils and macrophages producing cytokines, proteolytic enzymes, and free radicals. The main symptoms of IBD are bloody diarrhea, stomach pain and weight loss. The precise cause remains unclear however, evidence suggests it stems from a dysregulated immune response to commensal microbes in genetically predisposed individuals. Environmental factors, including diet, smoking, antibiotics, and other lifestyle influences, may also trigger or influence the condition. IBD is often diagnosed in early adulthood, but it can develop at any age; it affects both females and males equally.[11–14]

The two primary types of IBD are Crohn disease (CD) and ulcerative colitis (UC). CD and UC share some characteristics; however, studies have shown that genetic predisposition plays a more prominent role in CD than in UC. Despite that, it was observed that both diseases can occur within the same family, indicating that some susceptibility genes are shared in CD and UC.[15] In addition to that, for UC inflammation is typically confined to the colon and rectum, whereas CD can affect any part of the digestive tract, most commonly the terminal ileum.[13] More differences include endoscopic, clinical and histological features as well as the prevalence with UC being generally more common than CD, making it the predominant form of inflammatory bowel disease worldwide. Due to its higher prevalence, UC has been the focus of extensive research aimed at understanding its pathogenesis and improving treatment strategies.[16]

1.3. Ulcerative colitis

In Germany alone, 150.000 patients are affected by UC with a worldwide increase in incidence and prevalence during the last century.[15,17] North America, Australia and northern Europe have the highest incidence numbers worldwide, while eastern countries and countries in the southern hemisphere show the lowest, indicating that an industrialized lifestyle and western diet might influence the onset of UC.[16] The global incidence of UC can be seen in Figure 1. 1. Additionally, occurrence of previous gastrointestinal infections, like *Salmonella* or *Campylobacter*, have shown to double the risk of a patient developing UC, suggesting that the process of chronic inflammation can be triggered through previous acute intestinal infections.[18]

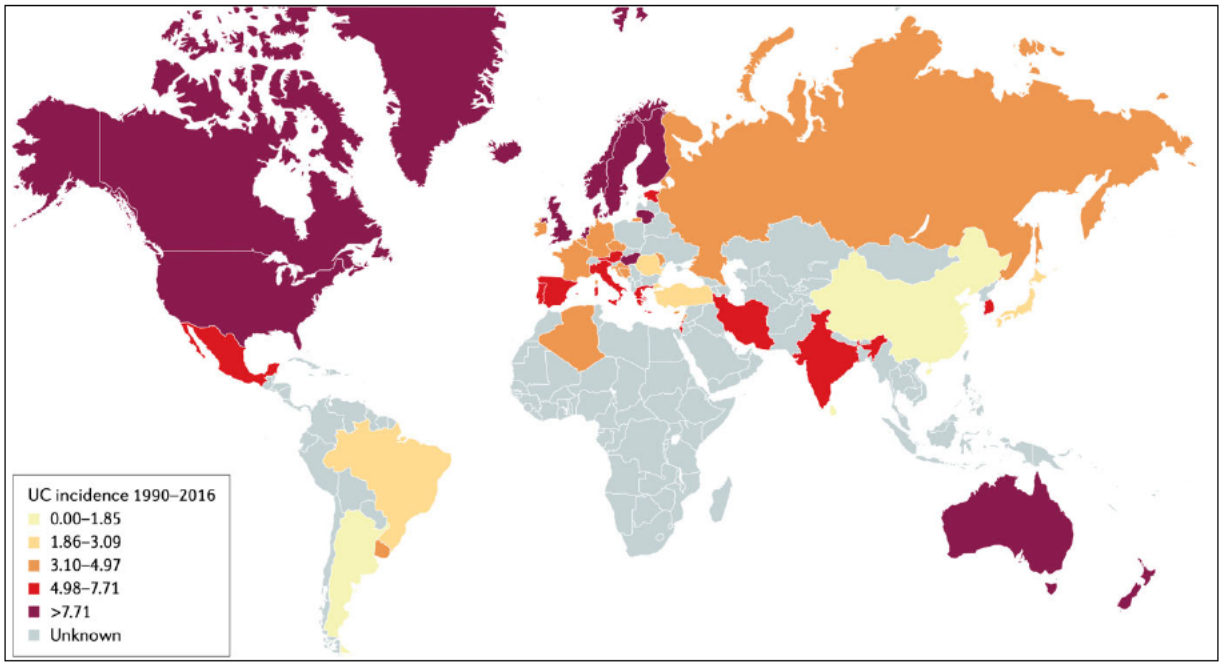

Figure 1. 1: Global prevalence of ulcerative colitis[18]
This figure shows the worldwide distribution of ulcerative colitis incidence from 1990 to 2016.

UC is diagnosed based on the clinical symptoms a patient is displaying, combined with findings from endoscopic examinations and histological analysis. Symptoms include bloody and/or mucous stool, diarrhea, abdominal pain, increased bowel movement frequency and tenesmus. An infectious (bacterial, viral, parasitic or fungal) or non-infectious (malabsorption or drug induced diarrhea) cause for the symptoms should be ruled out before a UC diagnosis is made.[13] In general, inflammation begins in the rectum and extends from distal to proximal colon in a continuous pattern. The inflammation may be visible through the formation of crypt abscesses, crypt distortion and epithelial cell death.[16,18] Over time, the destruction of the crypt epithelium can even lead to the collapse of the crypt structure, resulting in mucosal ulceration and fibrosis. The severity of UC can be classified based on the number of daily stools and the presence or

absence of systemic symptoms like fever. UC is treated depending on the severity of the disease. Mild to moderately severe UC is treated with anti-inflammatory drugs, like mesalzine. Another treatment option is oral corticosteroids. Severe cases of UC should be treated in the hospital where patients can receive corticosteroids intraveniously.[16,18] However, as of yet, there is no cure for UC.[19]

UC mainly affects the colon, but it has been observed that in up to 25 % of UC patients, the terminal ileum also shows inflammation.[20] Originally, this has been called backwash ileitis (BWI) based on the assumption that this is caused by a backwash of the colonic contents into the small intestine causing inflammation and an additional nutrient malabsorption. The pathogenesis of BWI however is complicated and some studies suggest it is rather Crohn's terminal ileitis and not caused by UC.[20] Either way, it has become part the standard procedure of a colonoscopy to biopsy the small intestine ileum (SII) in patients with suspected IBD as well and it is therefore important to include studying the SII when investigating UC.[20]

1.3.1. Pathophysiology of ulcerative colitis

The pathophysiology of UC is complex and not fully understood, however it is based on a disruption of the intestinal homeostasis allowing more luminal antigens to cross the epithelial cell barrier triggering an inflammatory cascade.[16,18] The more detailed process can be seen in Figure 1. 2.

The intestinal epithelial barrier and the mucosal layer act as the first line of defense, preventing harmful substances and pathogens from penetrating into the tissue below. In the first stages of the pathogenesis of UC this barrier becomes defective.[18] Studies have shown that the mucosal layer of the colon in UC patients is thinner than in healthy patients, which is the result of a reduction in mucin 2 production. A genetic deficiency may be the origin of this compromised barrier function, but environmental influences, such as changes in the microbiota, may also have an impact on the barrier breach. This assumption is strengthened by the fact that the addition of emulsifiers in food have led to the thinning of the mucosal layer in mice.[21,22]. The intestinal epithelium not only forms a physical barrier but also aids in host defense by generating antimicrobial peptides, like defensins, which also limit bacterial invasion. Due to the compromised epithelial barrier and mucinous layer, permeability is increased, leading to a defective regulation of tight junction protein expression. Overall, the disruption of the epithelial layer allows more luminal antigens, such as bacteria and toxins, to enter the lamina propria.[16] This stimulates the local, innate immune cells like macrophages, positive for F4/80, and

dendritic cells, changing their functional status to an activated phenotype via toll-like receptors (TLR). The NF-κB, or nuclear factor kappa-light-chain-enhancer of activated B cells, signaling pathway is activated in both cell types and the production of proinflammatory cytokines including tumor necrosis factor alpha (TNF-α) and interleukins IL12, IL23, IL6 and IL1β is increased. The NF-κB pathway has a pivotal role in regulating the production of those cytokines and therefore in the overall inflammatory and immune response making it a promising research target.[18,23]

Those cytokines are then presented to naive CD4 positive Th0 cells, promoting their differentiation into Th2 cells via the activation of IL4. The inflammatory response is further amplified as natural killer T-cells (NKT) produce IL13 which disrupt the epithelial barrier, increasing permeability and allowing even more bacterial products to cross. IL5 also enters the lamina propria, which contributes to the recruitment and activation of regulatory T-cells (Treg) that further propagate inflammation. Additionally, the development of IL9-producing Th9 cells exacerbates tissue damage by impairing tissue repair mechanisms, compromising tight junction integrity and, inhibiting cell proliferation, therefore reducing Ki-67 expression.[16,18,23]

In response to epithelial injury, damaged cells release IL33, which recruits more immune cells and enhances the Th2 response, further increasing inflammation. While anti-inflammatory mechanisms, such as the production of IL37, which reduces the production of TNF-α and IL-1β, aim to inhibit excessive immune activation, these pathways are often insufficient to restore equilibrium. Circulating T-cells carrying integrin-α4β7 are drawn to the site of inflammation through the mucosal vascular addressing cell adhesion molecule 1 (MAdCAM-1) on colonic endothelial cells, whose expression is further amplified in inflamed tissue. This mechanism leads to the infiltration of even more gut-specific T-cells into the lamina propria, further increasing chronic inflammation. Additionally, chemokines CXCL1, CXCL3, CXCL8, and CXCL10 attract extra leukocytes, strengthening the inflammatory cycle.[16,18,23]

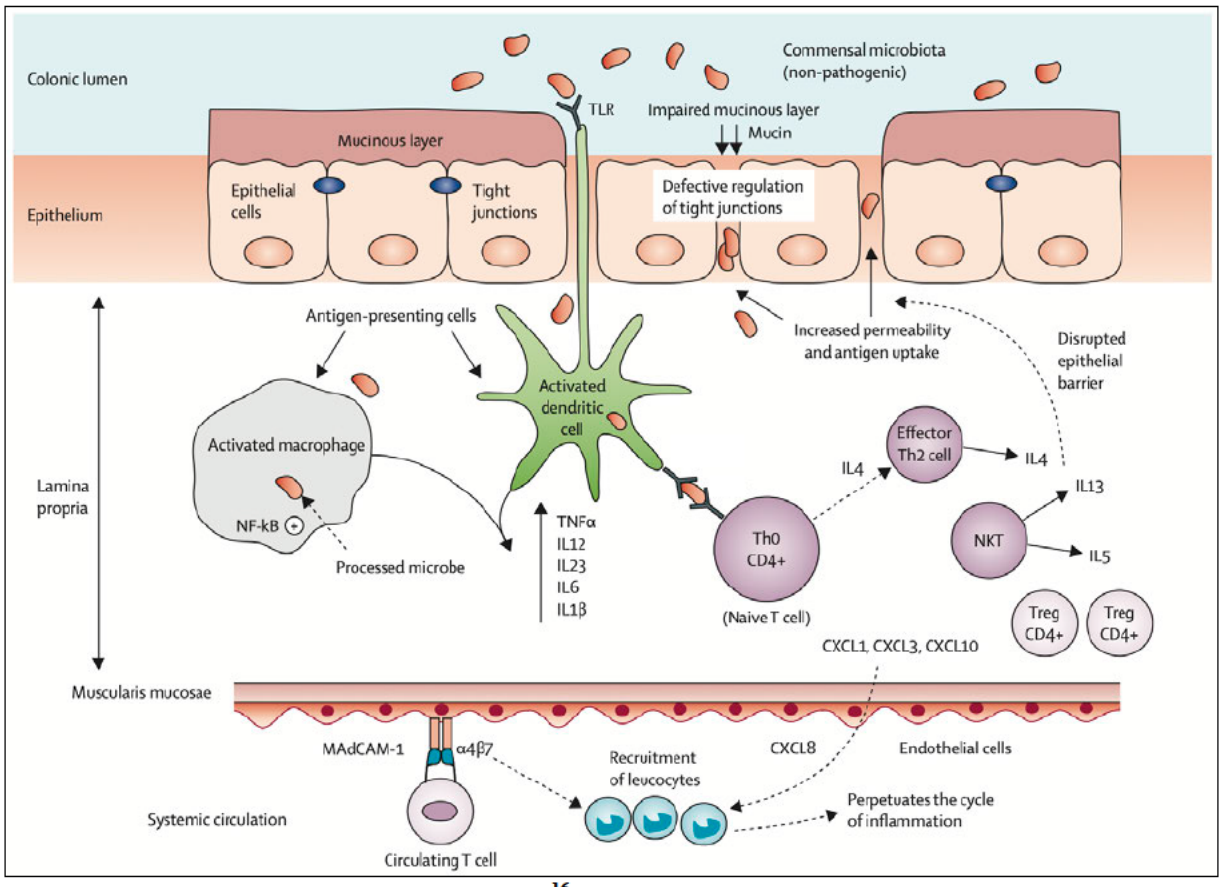

Figure 1. 2: Pathophysiology of ulcerative colitis[16]
The mucous layer is impaired, and the epithelial barrier is compromised, leading to a defective regulation of tight junctions. Luminal antigens enter the lamina propria. Macrophages and dendritic cells are activated via toll-like receptors (TLR). Pro-inflammatory cytokines IL12, IL23, IL6, IL1β and tumor necrosis factor α (TNFα). These are presented to naive CD4+ Th0 cells, promoting their differentiation into Th2 cells via the activation of IL4. Natural killer cells (NKT) produce IL13, which further destabilizes the epithelial barrier, and IL5 which recruits CD4 positive regulatory T-cells (Treg). Circulating T-cells carrying integrin-α4β7 are drawn to the site of inflammation through mucosal vascular addressing cell adhesion molecule 1 (MAdCAM-1). Chemokines CXCL1, CXCL3, CXCL8, and CXCL10 attract extra leukocytes, strengthening the inflammatory cycle. With IL=interleukin and Th=T helper cell

Despite significant advances in understanding the pathophysiology of UC, it is still, as mentioned previously, not fully understood. Key pathways, such as NF-κB signaling, have been identified as central regulators of immune activation and cytokine production, yet their broader role in perpetuating inflammation and tissue damage is still being explored. With the global incidence and prevalence of ulcerative colitis continuously increasing, the need for further research into its underlying mechanisms and potential therapeutic targets has become more and more urgent.[16] Developing a better understanding of these molecular mechanisms may open the door to new therapeutic approaches that target certain elements of the inflammatory cascade, like the NF-κB pathway.

1.3.2. Modelling colitis

To effectively study UC and develop improved therapeutic strategies, various models have been established to replicate its complex pathophysiology. The model systems include in vitro and in vivo models. In vitro models have the advantage of a better prediction of human clinical outcomes. Since in vivo models are based on animals, they show interspecies variability, including differences in cellular and molecular mechanisms as well as microbiota composition.[12] In the past decades in vitro systems have become more and more advanced, including nonepithelial components such as stroma, immune cells, and microbiota. This increased complexity allows for a more accurate representation of organ physiology and disease processes. In vitro systems include plate-based cell cultures, organoids and micro-physiological systems like organ-on-a-chip technologies. Advantages of in vitro systems include being able to perform high-throughput screenings as well as a reduced cost. In addition to that, it either offers a replacement to the employment of animals in experiments when using human based cell systems, or a reduction of employed animals when using animal cell-based systems, which both aligns with the 3R principles. Moreover, the integration of patient-specific cells through for instance organoids, allows for personalized models, enabling researchers to study UC in specific individuals or subpopulations and develop targeted therapies.[12,24]

Despite these advantages, in vitro models have inherent limitations. They present a simplified representation of the colon, making it challenging to replicate the full complexity and heterogeneity of the organ.[11,24] This simplification affects the ability to capture the complete pathophysiological mechanisms involved in UC, particularly when inflammation and immune responses are being studied. Existing models often focus on one or a few specific aspects of inflammation, potentially overlooking critical interactions and dynamics. Additionally, even the mechanisms that are modelled are often over simplified which can lead to a misunderstanding of the immune response.[11,24,25]

As of today, animal testing is indispensable for researching the pathophysiology and treatment options of UC. Animal based models allow the investigation of interactions between the immune system, microbiota, mucus layer and intestinal epithelium in a biologically complex and dynamic environment that closely mimics the physiological and immunological processes observed in humans. Additionally, animal models enable the study of disease progression over time, including the transition from acute to chronic UC. In addition, through genetic

engineering of the animal, certain pathways and their role in the development and regulation of the disease, can be closely investigated.[24,26]

There are over 60 animal models that have been established to study IBD with each having its advantages and disadvantages.[27] However, the most commonly used model for studying UC is dextran sulphate sodium (DSS) induced colitis.[19]

1.3.3. DSS induced UC model

It has been shown that the ingestion of DSS solutions induces inflammation in the colon of animals. It can be used to model both acute and chronic UC, with the severity of inflammation depending on the concentration of the solution, number of treatment cycles, the duration the DSS is being ingested and the species of animal that is used.[28] Most commonly rodents, specifically mice are used, with genetically modified animals allowing the investigation of certain pathways during the development of UC. The ingestion of 3 – 5 % DSS solutions leads to an infiltration of inflammatory cells into the lamina propria and submucosa, crypt abscesses, mucin depletion and the destruction of epithelium in the large intestine. The symptoms of the mice included bloody and loose stool and weight loss.[28,29]

Although the DSS model does not replicate the complexity and wide range of pathways of UC, it is an essential tool to investigate different factors involved in the pathogenesis as well as treatment options.[29] DSS treatment in immunocompromised mice, specifically T- and B-cell deficient mouse strains, also developed UC, showing that in this model the adaptive immune system does not play a role, which differs from the pathogenesis of UC in humans. Therefore the DSS model allows the studying of the innate immune response and its contribution to developing inflammation.[30]

Animals treated with DSS can experience pain, due to the symptoms caused by the inflammation of the colon including bloody diarrhea and abdominal discomfort.[31] Therefore, pain management in the DSS model is of importance, especially under the premise of following the 3R principles. It is therefore essential to explore whether the administration of analgesics can alleviate pain without interfering with the progression of UC or altering the underlying pathways being studied.

1.4. Transcription factor NF-κB

NF-κB is not a single gene but a family of transcription factors, that play a central role in regulating various cellular processes.[32] Discovered in 1986, it was initially identified for its role in B-cell activation. However, NF-κB has emerged as a central regulator of many cellular responses, including the immune response, cell death, cell proliferation, and through that also cancer development.[34] It consists of five proteins: RelA (p65), RelB, c-Rel, p50 (the precursor of p105), and p52 (the precursor of p100) that form hetero- or homodimers in various combinations. The composition of the dimer determines its binding affinity to DNA and the specific genes it activates.[32–34]

NF-κB has a central role in the inflammatory response, acting as a key transcription factor that controls the expression of numerous genes involved in inflammation. In the colon of IBD patients, NF-κB expression and activation is highly upregulated.[33,35] This shows its significant involvement in the development of UC, making it an important focus of research. Understanding the role of NF-κB not only allows for better understanding of the pathology of the disease but also holds promise for advancing the development of effective therapies. As mentioned in 1.3.1., the development of UC involves different cell types, many of which are regulated by NF-κB, and it is necessary to differentiate between the cell-specific effects of it. In macrophages, NF-κB activation increases the expression of pro-inflammatory cytokines TNF-α, IL1, and IL6. These cytokines contribute directly to tissue damage and amplify the inflammatory response by activating other immune cells. Additionally, NF-κB regulates the expression of IL12 and IL23, which are pivotal for T-helper cell differentiation, perpetuating inflammation. [33, 34,36]

In epithelial cells the role of NF-κB is more complex. On one hand, it has been shown that its activation promotes the recruitment of neutrophils to the inflammatory site via an induction through IL6.[35] However, another study has demonstrated anti-inflammatory functions of NF-κB in epithelial cells of the colon. Using a knockout mouse model, researchers found that the absence of NF-κB resulted in increased apoptosis of colonic epithelial cells, reduced production of antimicrobial peptides, and bacterial translocation into the mucosa. This defect subsequently initiated chronic inflammation in the colon, proving that NF-κB acts as a regulator of integrity and immune homeostasis in the epithelium.[36] In lamina propria fibroblasts, NF-κB activation is triggered through CD40 which is expressed by T-cells. This led to an increased production of pro-inflammatory cytokines like IL6 and IL8.[37]

Overall, the NF-κB transcription factor is a central regulator in the pathogenesis of IBD. Its role range includes increasing inflammation and immune activation to maintaining epithelial barrier integrity and immune homeostasis.[33] However, to fully know the functioning of NF-κB it is critical to understand its pathway.

1.4.1. Pathway of NF-kB

The pathway of NF-kB is split into the canonical and non-canonical pathways which are both depicted in Figure 1. 3. The canonical pathway is activated by stimuli such as pro-inflammatory cytokines like IL1β or TNF-α or cellular stress. Through various immune receptors including TLRs or TNF receptors (TNFRs) a signaling cascade unique to the stimulus is activated. The pathway induced by TNF-α is the most studied one and represents a typical canonical pathway.[36] A central step in that cascade is the activation of the IκB kinase (IKK) complex consisting of the catalytic subunits IKKα and IKKβ as well as the regulatory subunit NF-κB essential modulator (NEMO). Upon activation the IKK complex phosphorylates the inhibitory IκB proteins, leading to their degradation. The NF-kB dimers, typically consisting of p65 and p50, that were bound to the IκB are released and translocate into the nucleus through nuclear pores. In the nucleus, NF-κB binds to specific DNA sequences, known as κB sites, located in the promoter or enhancer regions of target genes. This binding initiates the transcription of genes involved in inflammation, immune response, and cell survival.[36,38]

The non-canonical pathway is initiated when specific receptors including B-cell activation factor receptors (BAFFR), CD40 or receptor activator for NF-κB (RANK) are activated. This allows for recruitment of adapter proteins that signal downstream to activate the NF-κB inducing kinase (NIK), a central kinase in this pathway. NIK activates IKKα which then phosphorylates p100. This phosphorylation triggers the processing of p100 into its active form, p52, which then pairs with RelB to form functional NF-κB heterodimers. Those dimers translocate to the nucleus, where they bind to κB binding sites in the promoters of target genes.[36,38]

While the canonical pathway provides a rapid and transient response to a broad range of stimuli, the non-canonical pathway reacts to a selection of cell-differentiating or developmental stimuli and acts slower but sustained. Together, these pathways show the versatility and complexity of NF-κB signaling, underscoring its importance in both health and disease.[33]

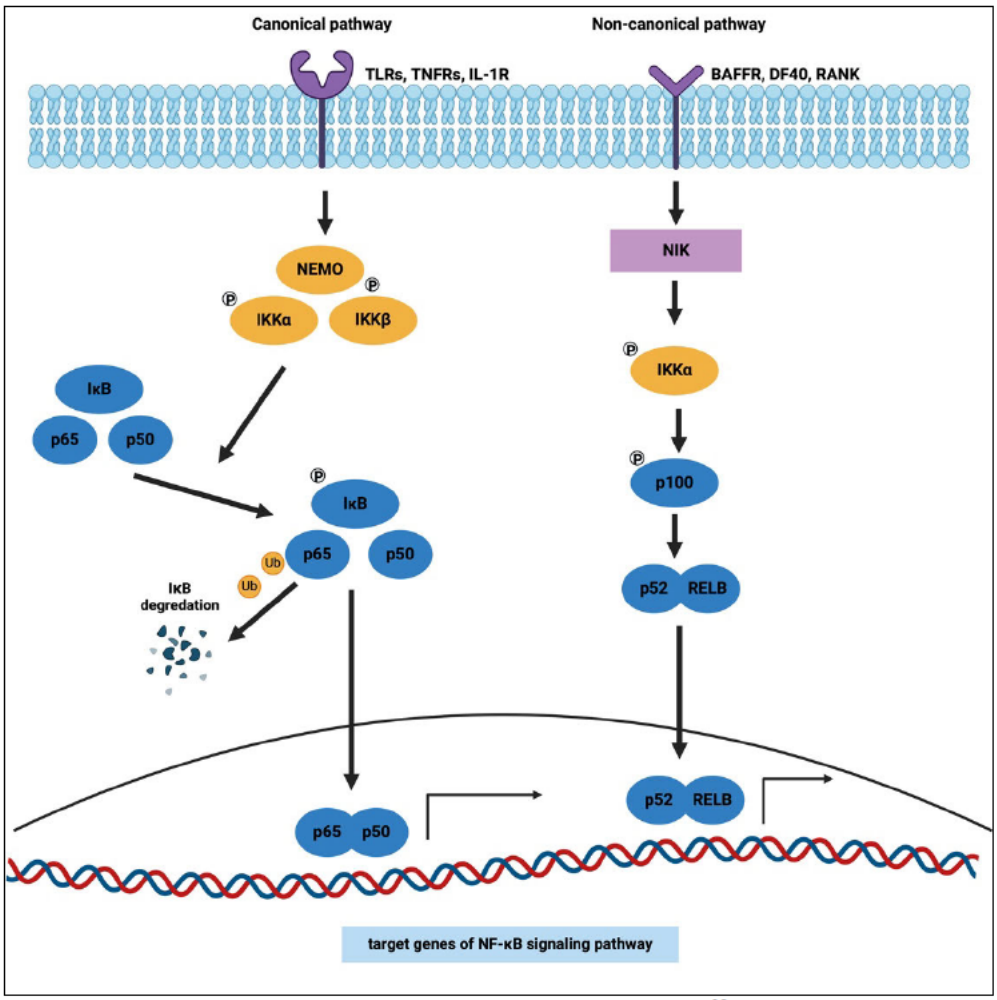

Figure 1. 3: The NF-κB signaling pathway (adapted in BioRender from [38])
The canonical pathway is induced by a ligand binding to TLRs, TNFs or IL-1Rs. A signaling cascade is activated. The IκB kinase (IKK) complex consisting of the catalytic subunits IKKα and IKKβ and the regulatory subunit NF-κB essential modulator (NEMO). The IKK complex phosphorylates the inhibitory IκB proteins, leading to their degradation. The NF-kB dimers, consisting of p65 and p50, that were bound to the IκB are released and translocate into the nucleus through nuclear pores. There, they bind to target genes of the NF-κB signaling pathway. The non-canonical pathway is initiated with the activation of B-cell activation factor receptors (BAFFR), CD40 or receptor activator for NF-κB (RANK). The NF-κB inducing kinase (NIK) is activated, which activates IKKα which then phosphorylates p100. This phosphorylation triggers the processing of p100 into its active form, p52, which then pairs with RelB to form functional NF-κB heterodimers. Those dimers translocate to the nucleus, where they bind to κB binding sites in the promoters of target genes.

1.5. Artificial intelligence in science

The developments in artificial intelligence (AI) have created new possibilities to optimize experimental research and have transformed the way experiments are set up, conducted and analyzed. There are many plans for the implementation of AI into scientific research; self-driving laboratories, generative AI replacing human participants and creating discoveries entirely based on in silico simulations and predictive modeling. This promises to transform research and can offer a solution to longstanding limitations including time and financial

constraints as well as cognitive overload from all the available data, allowing an increase in productivity and the most optimal use of the available resources.[39,40]

One use of AI is to deal with the ever-growing number of scientific literature. PubMed alone, a widely used research engine for biomedical literature, contains over 37 million articles as of August 2023, with roughly a million more added each year. This volume of information often exceeds human processing capabilities, which the use of AI can address by rapidly analyzing, organizing and extracting important information. These results can be used to optimize the design and set-up of experiments or assist in the creation of entirely new hypothesizes. A drawback of this method is that AI does not assess the quality of publications, which is a big problem because the majority of scientific papers are not reviewed.[41,42] AI can also be used to improve data collection and simulation. Certain AI methods, particularly generative models, can create synthetic datasets and simulate experimental conditions or outcomes. This allows for testing hypotheses and study complex phenomena with reduced or even without physical experimentation.[39,40,42]

Using AI also helps in the alignment of the experimental design with the 3R principles. As mentioned before, science still regularly relies on animal testing. Through the prediction of experimental outcomes via deep learning models, the number of employed animals can be reduced. Furthermore, AI can be used to refine the experiment and optimize the conditions under which the animals are used, such as the pain management during treatment processes.

1.5.1. PEDL+

In 2020, a model to predict protein-protein associations (PPAs) from biomedical publications was developed by a group at the Max Delbrück Center (MDC). This tool is called PEDL standing for PPA Extraction with Deep Language. PEDL is based on pretrained language models like SciBERT and combines those with distant supervision, allowing to source more data compared to when relying solely on manually labelled annotations. PEDL sources large protein pair datasets from resources like the Protein Interaction Database and matches them to biomedical texts. Besides predicting the PPAs, PEDL also identifies and counts specific text spans that name these associations, increasing transparency and verifiability.[43,44]

In 2023, PEDL was improved and reimplemented as PEDL+, making it easier to use, scalable and customizable. Besides PPAs it also allows the extraction of different types of chemical-protein relations. PEDL+ is freely available and was used to identify the best fitting

analgesic for the DSS induced UC mouse model.[45] Here, the focus was on selecting analgesics that provide effective pain relief while having minimal interference with the NF-κB pathway and the inflammatory response.

In the initial step, prior to conducting the main PEDL+ search, analgesics were identified through resources such as national veterinary societies, veterinary manuals, and university animal welfare databases. This preliminary selection focused on analgesics with established efficacy in pain relief, which eliminates the need for extensive safety testing and facilitates their implementation in animal research. Subsequently, a set of target genes was defined, including members of the NF-κB family - RelA (p65), RelB, cRel, p50, and p52 - along with upstream kinases and other mediators involved in signaling pathways.

Following this preparation, the primary PEDL+ search was conducted. Gene and drug lists were put into the program, which analyzed over 30 million abstracts and four million full texts from biomedical publications to predict association types between proteins and drugs. Two separate runs were performed, one with analgesics and human genes, and another with analgesics and mouse genes. Each drug was scored based on the number of publications supporting its interactions with target genes and the frequency of relevant text passages. A higher score indicated stronger evidence of drug-target interactions. However, since older drugs naturally appeared in more publications, normalization was applied to correct for publication bias. The scores were adjusted according to the number of years since the compound was first described, ensuring that recently identified analgesics didn't have disproportionately lower scores.

As a result of this process, 18 analgesics achieved a normalized score of zero, indicating the strongest potential for use in the colitis model. Notably, Tramadol and Paracetamol, both frequently used in colitis studies and recommended by the Landesamt für Gesundheit und Soziales (LAGeSo), received high scores and were therefore selected as positive controls. To further validate these findings, PubChem was used to assess whether the absence of evidence for the 18 best scoring drugs was reasonable. For 16 of these analgesics, no evidence of chemical-target interactions was identified, supporting the validity of the PEDL+ predictions.

In the final step, SuperPred and SwissTargetPrediction were employed to predict interactions based on structural similarity. For eight of the analgesics, no targets related to NF-κB signaling were detected, however most of these fell into the category of nonsteroidal anti-inflammatory drugs (NSAIDs) and were therefore excluded. Among the remaining candidates were two opioids meperidine (pethidine) and piritramide, along with amantadine, a member of the

adamantane class. Due to the severe side effects associated with meperidine, it was excluded. Consequently, the final selection included Amantadine and Piritramide, in addition to Tramadol and Paracetamol as positive controls. This entire search process was conducted by Prof. Dr. Jana Wolf and her group from MDC.

The deep learning based PEDL+ search has allowed for a great improvement of the preclinical research. The systematic and data-driven pre-selection of analgesics eliminated the need to test many compounds directly on animals. By searching through a big number of publications, more than a human could in such a short time span, PEDL+ allows the focus to be only on the most promising candidates. This approach not only saves time and resources but also aligns with the 3R principles. It reduces the number of animals required to test the applicability of these drugs in the DSS induced UC model, while also enabling the refinement of animal welfare by effectively alleviating pain in the animals that are used.

1.6. Pain and analgesics in experimental animals

Pain is a common but complex sensory perception, which plays a vital role as an alarm signal in the body. It can be triggered from different sources and involves many systems in the body. Despite pain being mainly associated with humans, many if not all vertebrates are believed to experience pain as well.[46] Pain is associated with many physiological and behavioral responses and can have an impact on experimental data, therefore potentially decreasing the reliability and reproducibility of experimental outcomes. In addition to that, pain can lead to a decreased food and water consumption resulting in weight loss, metabolic disturbances, and impaired recovery, which may further confound experimental results and compromise the overall welfare of the animals. Yet, sometimes pain is part of the experimental model because it is a part of the disease process and can mimic clinical symptoms observed in humans.[46,47] Despite that, scientists have an ethical obligation to ensure the humane treatment and wellbeing of the animals used in their research. This responsibility includes minimizing pain and distress and implementing measures following the 3R principles.

A possible tool to alleviate pain for the animals during an experimental treatment is the use of analgesics, however this also presents several challenges. The right analgesic needs to be selected to effectively relief pain with minimal influence on the pathways and processes that are being studied. Many commonly used analgesics, such as NSAIDs, can influence immune

responses or other physiological functions, potentially affecting the experimental outcomes. Also, species differences in metabolism can lead to variations in the effectiveness and side effects of a drug. Therefore, selecting and testing an appropriate analgesic for the specific animal species and experimental model is a crucial part of experimental design.[48–50] The following analgesics were selected using the deep learning based tool PEDL+, with paracetamol and tramadol being used as positive control to gage the effectiveness of the deep learning search and amantadine and piritramide being the most promising candidates according to the program.

1.6.1. Paracetamol

Paracetamol, also known as acetaminophen, is one of the most widely used analgesic and antipyretic drugs worldwide. It was first discovered in the 1880s by A. Chan and P. Heppa and introduced to the market in the 1950s as a prescription drug by the company McNeil Laboratories. Nowadays, paracetamol is a non-prescription drug, commonly used to alleviate mild to moderate pain or fever. The exact mechanism of action of paracetamol has not been fully understood, despite it being already discovered in the 19th century. It has similar analgesic and antipyretic properties to NSAIDs, yet it typically does not show anti-inflammatory properties.[51] However, several studies have suggested that paracetamol may influence the inflammatory response, particularly through its ability to reduce synovial effusion and tissue volumes in patients with knee osteoarthritis, as well as its role in inhibiting cyclooxygenase enzymes.[52,53] Furthermore, it has been observed that Paracetamol has an influence on the NF-κB pathway, making it the ideal positive control for this experiment.[54,55]

1.6.2. Tramadol

Tramadol was firstly synthesized by the German company Grünenthal, patented in the 1970s, and is nowadays a widely used analgesic available in a variety of formulations including tablets or drops for oral and solutions for IV, IM or SC administration. Its analgesic potency is about 10 % of that of morphine and is as a weak opioid employed for moderate to severe pain. However, compared to other opioids, tramadol has the advantage of a decreased respiratory depression.[56–58] It has a dual mechanism of action, meaning it exerts its analgesic effects primarily through weak affinity for μ opioid receptors and inhibition of norepinephrine reuptake while increasing serotonin secretion. Tramadol is a racemic mixture, meaning it consists of two enantiomers, both of which have different opioid binding affinities and different mechanisms of action.[59] It has been proven that tramadol shows anti-inflammatory properties as well as an influence on the activation of NF-κB.[34,56,58,60]

1.6.3. Amantadine

Amantadine, or adamantan-1-amin, is an adamantane derivate and was first developed in the 1960s by the company DuPont. It is usually formulated as capsules or tablets for oral administration and is commonly used to treat Parkinson's disease or type A influence virus induced flu, due to its antiviral properties.[61,62] The primary mechanism of action of amantadine involves antagonism of N-methyl-D-aspartate receptors, which play a crucial role in pain transmission and central sensitization. By inhibiting these receptors, amantadine may reduce the amplification of pain signals, thereby alleviating pain. Some clinical studies have investigated its efficacy in pain management and shown promising results. However, further research is necessary to fully understand the analgesic potential of amantadine. [63,64] It has been reported that at higher doses amantadine has led to a decrease of pro-inflammatory cytokines like IL1β, IL6 or TNF-α which could also indicate an influence on the NF-κB pathway. This however still needs further investigation.[62,65,66]

1.6.4. Piritramide

Piritramide, a synthetic opioid analgesic, was first synthesized in 1960 by Paul Janssen and introduced to the pharmaceutical market in the early 1970s. It is a pure μ opioid receptor agonist and provides effective pain relief in both acute and chronic pain and is used particularly in postoperative settings. Piritramide is a member of the piperidine class of opioids, which also includes other well-known drugs like fentanyl and pethidine. In Germany, piritramide is widely used, however in some countries including the USA and UK it is not commercially available. It can only be administered parenterally, which allows for rapid onset of action. Since piritramide is an opioid, it could have an influence on the NF-κB pathway. While some opioids have been shown to impact inflammation or the NF-κB pathway, there is currently no direct evidence demonstrating that piritramide does so too.[67,68] Further research is needed to clarify whether piritramide exerts any immunomodulatory effects similar to other opioids.

1.7. Aim of this project

Animal experiments are still necessary to model UC due to its complexity as a multi organ disease involving interactions between the immune system, intestinal epithelium, and microbiota. Following the 3R principles, this project builds on a deep-learning-based search to identify the best fitting analgesics for the DSS induced UC model and validate the findings of that search through in vivo experiments. Using the PEDL+ model, amantadine and piritramide were identified as the most promising candidates for a minimal influence on inflammation and the NF-κB pathway, paracetamol and tramadol were identified as having a high impact and therefore selected as positive controls. In the first part of the project, it was assessed whether the selected analgesics, independently trigger inflammation. Based on these findings, the most suitable analgesic was tested in a DSS-induced UC mouse model to evaluate its effects under inflammatory conditions. Analyses included pain evaluation using the Mouse Grimace Scale, Hematoxylin and Eosin (H&E) staining to assess histopathological alterations as well as immunofluorescence staining to examine immune cells, NF-κB activation, and intestinal epithelial cell changes. Besides the effect on the colon, also changes in the SII were evaluated.

2. Materials

In this chapter, the chemicals, materials and devices used during the experiments are listed and the applied methods are explained. A laboratory with basic equipment is assumed. The mouse treatment as well as all the laboratory work was carried out at the MDC in Berlin Buch. The microscopy was performed at the Charité Virchow Clinic at the department of hepatology and gastroenterology in Berlin Wedding.

2.1. Chemicals and materials

Table 2. 1: Used chemicals and materials

Name	Company	Specification
Acetic acid	Carl Roth	6755
Adhesion slides	Fisher Scientific	10149870
Agarose	Bioline	BIO-41025
Citric acid monohydrate	Carl Roth	3958
Cover glasses	Carl Roth	H878
Dextran sulfate sodium salt (DSS)	MP Biomedicals	12871781
DirectPCR Lysis Reagent	Viagen Biotech	402-E
DNA marker 100bp	Biosell	BS.CJ771.20-10
Entellan™	Sigma-Aldrich	107960
Eosin	Sigma-Aldrich	HT11023
Ethanol, ≥ 99,8 %, denatured	Carl Roth	K928
Ethidiumbromid solution 1 %	Carl Roth	2218
Formalin solution, neutral buffered, 10 %	Sigma-Aldrich	HT501128
GoTaq® DNA Polymerase	Promega	M3001
Hämatoxylin	Carl Roth	X903
Hydrochloric acid	Carl Roth	4625
ImmEdge® Hydrophobic Barrier Pen	Vector Laboratories	VEC-H-4000
Immu-Mount™	Fisher Scientific	10662815
Mikrotom disposable blades	Fisher Scientific	12191830
neoLab® embedding cassettes for biopsies	neoLab Migge	70018
Normal donkey serum	BIOZOL	LIN-END9010
Nuklease-free water	Fisher Scientific	PR-P1193
Paraplast Plus®	Carl Roth	X881
PBS (10x), pH 7.4	Thermo Fisher	70011044
PBS, Phosphate Buffered Saline, 10X	Fisher Scientific	BP39920
Proteinase K, recombinant	Roche	3115836001

Name	Company	Specification
ROTI®Histol	Carl Roth	6640
Sodium chloride	Carl Roth	3957
TAE - buffer (50X)	APPLICHEM	A1691
tri-sodium citrate dihydrate	Carl Roth	3580
TRIS	Carl Roth	4855
TRIzol™ reagent	Thermo Fisher	15596018
Tween® 20	Carl Roth	9127
UltraPure™, DNase/RNase-free ddH_2O	Fisher Scientific	11538646
UltraPure™ 0.5 M EDTA, pH 8.0	Thermo Fisher	15575020
Xylol (Isomer)	Carl Roth	9713

2.2. Antibodies

Table 2. 2: Used primary antibodies

Target protein	Host	Company	Specification
CD3	Mouse	Dako	M7254
F4/80	Rabbit	Cell Signaling	70076S
GFP	Goat	Abcam	ab6673
Ki67	Rat	Thermo Fisher	14-5698-80
Mucin-2	Rabbit	Santa Cruz Biotechnology	sc-15334

Table 2. 3: Used secondary antibodies

Antibody (Alexa fluor conjugate)	Company	Specification
DAPI	DAKO	D9542
Donkey anti-goat (488)	Thermo Fisher	A11055
Donkey anti- goat (546)	Thermo Fisher	A11056
Donkey anti- goat (647)	Thermo Fisher	A21447
Donkey anti-mouse (488)	Thermo Fisher	A21202
Donkey anti- mouse (546)	Thermo Fisher	A10036
Donkey anti- mouse (647)	Thermo Fisher	A31571
Donkey anti-rat (488)	Thermo Fisher	A21208
Donkey anti- rat (647)	Thermo Fisher	A78947
Donkey anti- rabbit (488)	Thermo Fisher	A21206
Donkey anti- rabbit (546)	Thermo Fisher	A10040
Donkey anti- rabbit (647)	Thermo Fisher	A31573

2.3. Buffers and solutions

Table 2. 4: Used buffers and recipes

Description	Reagent	Amount
Acetic acid water	Acetic acid (100 %)	50 µl
	ddH_2O	9.95 ml
Citrate buffer	Solution A	27 ml
	Solution B	123 ml
	ddH_2O	1350 ml
Eosin solution	Eosin (freshly filtered)	7.96 ml
	Acetic acid (100 %)	40 µl
Donkey blocking solution	1x TBST	9 ml
	Normal donkey serum	1 ml
PBS	PBS (10x)	100 ml
	ddH_2O	900 ml
Solution A (acidic)	Citric acid monohydrate	21,01 g
	ddH_2O	1000 ml
Solution B (alkaline)	Sodium citrate	25,41 g
	ddH_2O	1000 ml
TAE buffer	Tris	242 g
	Acetic acid (concentrated)	57,1 ml
	0.5 M EDTA (pH 8)	100
	ddH_2O	843 ml
10x TBS	Tris	60.6 g
	Sodium chloride	87.7 g
	Hydrochloric acid	Until pH = 7.6 (around 50 ml)
	ddH_2O	Fill up to 1 L (around 950 ml)
TBST	10x TBS	100 ml
	Tween20	1 ml
	ddH_2O	900 ml

2.4. Analgesics

Table 2. 5: Used analgesics

Name	Specification	Company
Amantadine	Amantadinhydrochloride 100 mg Filmtabletten	ratiopharm
Paracetamol	Paracetamol-ratiopharm Lösung 40 mg/ml	ratiopharm
Piritramide	Dipidolor 7,5 mg/ml	Piramal Critical Care BV
Tramadol	Tramal 100 mg/ml Lösung, Tramadolhydrochlorid	Grünenthal GmBH

2.5. Devices

Table 2. 6: Used devices

Name	Description	Company
Axio Observer 7	Microscope	Zeiss
HM 355S Microtome	Histological tissue sections	Fisher Scientific
ProFlex™ PCR-System	PCR	Applied Biosystems
Quantum ST5 v16.12	Gel documentation	Vilber Lourmat
Seven Compact S220	pH meter	Mettler-Toledo
T3000	PCR	Biometra
Thermomixer comfort	Cell lysis	Eppendorf

2.6. Mouse line

A NF-κB reporter mouse model was used for the experiments in this project (*villinCRE x iκB alpha fl/fl igk-EGFP-3*/*OLA* and *villinCRE x loxP (loxPdeltaN) igk-EGFP -3/OLA*, in this studie called kEGFP mice) This allowed the cell-specific identification of NF-κB activation in different tissues. It was designed with the NF-κB binding sites placed upstream of the enhanced green fluorescent protein (EGFP) gene, allowing for EGFP expression as a direct response to NF-κB activation. The mice were kept at MDC in Berlin Buch and taken care of by trained animal caretakers.

3. Methods

3.1. Genotyping of mice

3.1.1. Tissue collection and DNA extraction

The mice were identified using an ear-punching system, where unique identification numbers were assigned based on the position of ear biopsies punched into their ears. The tissue removed during this process was collected and put into labeled 1.5 ml microcentrifuge tubes. This procedure was performed by trained animal caretakers from the MDC. The tubes were stored at -20 °C until further processing. 100 µl of the lysis reagent directPCR (Ear) and 1 µl of proteinase K was added into each tube. The samples were incubated overnight at 52 °C to ensure complete tissue digestion. The next day the Proteinase K was inactivated by heating the samples at 85 °C for one hour. The resulting lysates were used directly for PCR without further purification and stored at -20 °C.

3.1.2. PCR amplification

Genotyping PCR was performed using GoTaq DNA polymerase to identify the presence of EGFP. The PCR master mix was prepared by combining 5 µl of GoTaq polymerase, 0.1 µl of upstream primer (5'- AGT GAG GGA GCA GAA GGC -3'), 0.1 µl of downstream primer (5'- GGC TTC TTT GAG GGC TCG -3'), and 5 µl of nuclease-free water per reaction. For each PCR reaction, 10 µl of the prepared master mix was aliquoted into individual PCR tubes, followed by the addition of 0.4 µl of the extracted DNA sample. A positive control as well as just the master mix as the negative control were also added into individual PCR tubes. PCR amplification was conducted using the appropriate thermal cycling program specific to the EGFP target gene on a PCR machine, see Table 3.1.

Table 3.1 PCR protocol for genotyping

Gene of interest	Temperature	Time	Number of cycles
EGFP	94 °C	2 min	1
	94 °C	30 s	42
	62 °C	30 s	
	72 °C	40 s	
	72 °C	10 min	1
	4 °C	30∞	

3.1.3. Gel electrophoresis

PCR products were analyzed using gel electrophoresis with 2 % agarose gels. Each gel was prepared by dissolving 2 g of agarose powder in 100 ml of 1X TAE buffer, followed by the addition of 2 µl of ethidium bromide for DNA staining. After the gel was cast and allowed to cool, 7 µl of each PCR sample, along with a 100 bp DNA marker as ladder and the controls were pipetted into the respective chambers of the gel. Electrophoresis was performed at 70V for around 45 minutes. DNA bands were visualized under UV light and the respective height of the DNA band in each sample was compared to the positive control to confirm the presence of the targeted gene location.

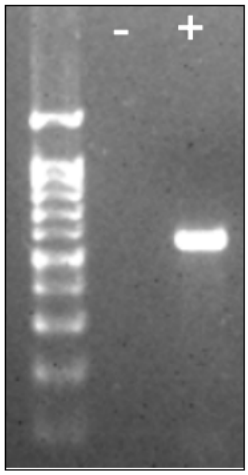

Figure 3. 1 Result of gel electrophoresis
The DNA 100 bp ladder is shown, as well as a negative (-) and positive (+) sample for EGFP.

3.2. Mouse treatment

Following genotyping, five mice were selected for each treatment group based on the presence of EGFP-positive individuals, with two to five EGFP-positive mice included per group. The gender of the mice was randomized and was not a factor in the experimental design. The mice used in the experiment were of similar age between the groups, although the age was not a specific focus of the study. Efforts were made to ensure that each group contained mice of comparable age. Each treatment lasted over the period of five days. After this the mice were sacrificed by cervical dislocation. All animal work was approved by LAGeSo, ethics approval: G0175-23.

3.2.1. Analgesic mouse treatment

In the first part of the experiment, five groups with five mice each were set up. The groups consisted of untreated controls, Tramadol, Paracetamol, Amantadine, and Piritramide treatments. Tramadol, Paracetamol, and Amantadine were administered orally via the mice's drinking water. The concentration of paracetamol was 200 mg/kg bodyweight, and of amantadine 2 mg/kg bodyweight all daily, based on an average mouse weight of 23 g and an estimated daily water intake of 5.8 ml per mouse. Tramadol was given to the drinking water with a concentration of 0.1-1 mg/ml. Piritramide was administered intraperitoneally at a final concentration of 10 mg/kg of body weight per mouse. The mice were weighed before each administration and the volume of the drug individually adjusted. The injections were performed intraperitoneally by trained animal caretakers on days zero and three of the treatment period. The treatments are visualized in Figure 3. 2.

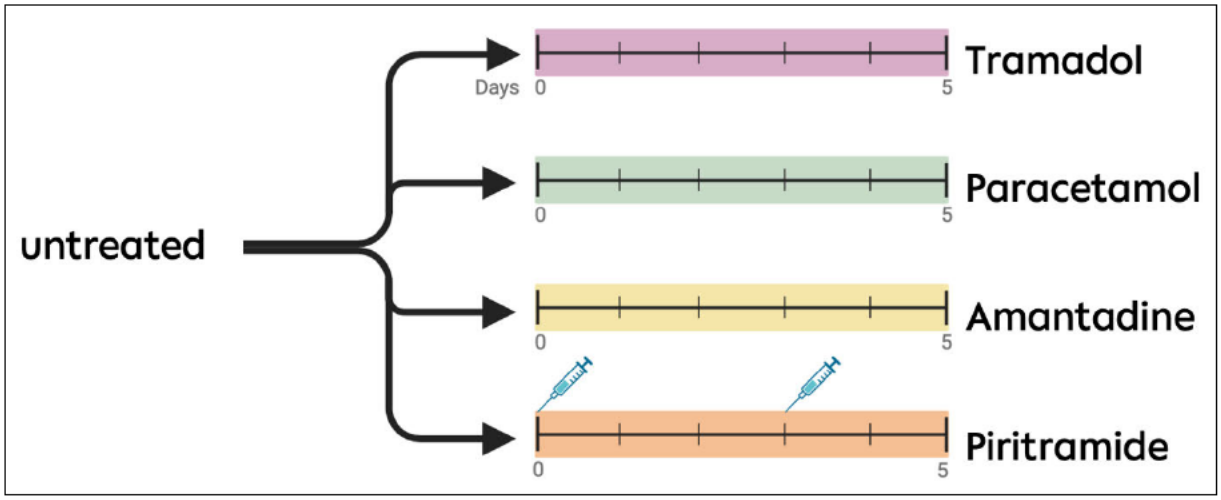

Figure 3. 2: Analgesic treatment groups

3.2.2. Colitis mice with and without analgesic

Two groups of mice were used in this experiment. Group one, consisting of three mice, served as the colitis control group. These mice were treated with 3% DSS in their drinking water for the duration of the experiment. Group two, consisting of five mice, received a combined treatment of Amantadine at a concentration of 2 mg/kg body weight and 3% DSS in their drinking water. The treatments for both groups lasted for five days and are visualized in Figure 3. 3.

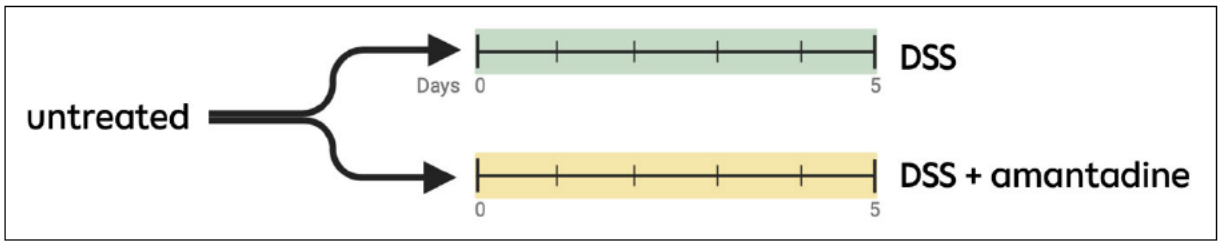

Figure 3. 3: DSS and DSS + amantadine treatment groups

3.3. Organ collection and processing

After sacrificing the mice, the colon and SII were dissected and cleaned in ice-cold PBS. The intestines were then prepared as Swiss rolls and placed upright in paraffin embedding boxes, which were closed to secure the tissue. The tissue was fixed in 10 % formalin solution at 4 °C overnight while gently shaking. After fixation, the intestinal pieces were washed twice for a few minutes in PBS while shaking, followed by a wash in 70 % ethanol for 10 min at room temperature. The tissue was then incubated in 70 % ethanol for at least 24 hours at 4 °C.

Freshly filtered paraffin was prepared in a 60 °C incubator. Dehydration was performed at room temperature using a series of ethanol solutions: 30 min in 80 % ethanol, followed by 30 min in 90 % ethanol, and then 60 min in 96 % ethanol. The samples were washed again for 30 min in 96 % ethanol, followed by two 30 min washes in 100 % ethanol. The tissue was then incubated for 15 min in a 1:1 mixture of ROTI® Histol and 100 % ethanol. Afterwards, the tissues were incubated in ROTI® Histol for 60 min, followed by another 30 min incubation in ROTI® Histol. Once dehydrated, the samples were allowed to dry for 4 min on a sheet under the hood. The tissues were placed into liquid paraffin in a glass box in a 60 °C incubator overnight. The Swiss rolls were embedded into paraffin using metal casings. The samples were cured at 4 °C until hard. Histosections were prepared with a thickness of 4 µm using a microtome and put onto glass slides. The slides were dried on a heating plate at 37 °C overnight.

3.4. Hematoxylin and eosin (H&E) staining

For H&E staining, the histosection slides were first rehydrated by performing a series of solvent washes. The slides were immersed in xylol three times for five minutes each, followed by two washes in 100 % ethanol for five minutes each. The slides were then washed once in 96 % ethanol for ten minutes, followed by a five minute wash in 70 % ethanol. Finally, the slides were rinsed for one minute in ddH_2O. The staining process began with the application of Hematoxylin Gill II for five minutes, ensuring that it was filtered before use. The slides were then briefly washed in acetic acid water and followed by a quick rinse in distilled water. The slides were then washed with flowing tap water for six minutes to thoroughly wash out the hematoxylin. Next, the slides were stained with eosin solution for 90 seconds, ensuring that the solution was freshly prepared and filtered before use. Afterward, the slides were briefly rinsed with 70 % ethanol, twice with 96 % ethanol and three times with 100 % ethanol. The samples were then covered with Immu-Mount or Entellan and cover slips.

Hematoxylin attaches to negatively charged components of the tissue, such as nucleic acids. It has a blue or purple color, and the intensity of the color depends, besides the incubation time, also on the amount of DNA and RNA present. Eosin stains proteins nonspecifically, therefore the cytoplasm, extracellular matrix, and other components are stained in varying shades of pink or red. This allows for the detailed visualization of tissue architecture and cellular structures.[69]

3.5. Immunofluorescence staining

Immunofluorescence staining was performed to visualize protein expression in tissue sections using specific primary and fluorescently labeled secondary antibodies. The protocol began with rehydration of the histological slides. The slides were immersed in ROTI® Histol for ten minutes twice, followed by two five-minute washes in 100% ethanol. This was followed by sequential five-minute washes in 96 %, 90 %, 80 %, 70 %, and 50 % ethanol. Afterward, the slides were washed in distilled deionized water for five minutes and then rinsed in 1xTBST buffer for another five minutes. For epitope demasking, 1.5 liters of citrate buffer at pH 6 were prepared. The buffer was preheated in a pressure cooker, the slides were submerged in the hot buffer. The tissue sections were cooked for 15 min and then cooled to room temperature. The tissue sections were encircled with a hydrophobic barrier and washed for five minutes with 1xTBST buffer. 50 µl of donkey blocking solution was added onto each sample and incubated

for 30 min at room temperature. The first antibody mixture was prepared by diluting specific primary antibodies in 1xTBST buffer, with a dilution factor of 1:50. The blocking solution was removed, and 50 µl of the antibody mixture was added per slide, ensuring full tissue coverage. The slides were incubated overnight at 4 °C. The following day, the slides were washed three times for 10 min each in 1xTBST buffer. A secondary antibody mixture was prepared by diluting specific secondary antibodies and DAPI in 1xTBST buffer, with a dilution factor of 1:1000. The prepared mixture was applied with 50 µl per tissue, and the samples were incubated in the dark for 60 min. After incubation, the slides were washed three times for 10 min each in 1xTBST buffer under dark conditions. The samples were mounted with Immu-Mount and a cover slip. The slides were stored at 4 °C until analysis.

The employed antibodies include CD3, F4/80, Ki67, Muc2 and EGFP. CD3 is a marker used for the identification of T lymphocytes as it is part of the T-cell receptor complex.[70] F4/80 is a unique marker for murine macrophages because those express a specific antigen that the F4/80 antibody binds to.[71] Ki67 is a protein expressed only by proliferating cells and is therefore a marker for cell proliferation and an indicator for stem cells.[72] Muc2 is the main mucin in the small and large intestine and forms a protective layer. It is expressed specifically in goblet cells and can be used as a marker for those.[73] The fluorescent marker EGFP is used in the employed mouse model to visualize NF-κB activation and allows the localization of cells in which the NF-κB pathway is active.

3.6. Microscopy

Microscopic analysis was performed on the prepared tissue sections using a Zeiss Axio Observer 7 microscope with immunofluorescence and brightfield imaging capabilities. For H&E-stained samples, the brightfield mode was used to assess histological features. For immunofluorescence-stained sections, fluorescence imaging was employed, allowing the detection of specific fluorescence signals. The channels used for imaging were 647 nm, 555 nm, 488 nm, and 461 nm (DAPI), corresponding to the emission spectra of the fluorescent dyes applied during staining. Magnification was 20x with a numerical aperture of 0.8. The exposure was set manually and adjusted individually for each sample to optimize image quality. After microscopy, the slides were stored at 4 °C.

3.7. Analysis

The analysis of the data obtained from H&E and Immunofluorescence staining was performed using a combination of software tools, including ImageJ Fiji and Zeiss Zen Light for image processing and GraphPad Prism 10 for the generation of figures and statistical analysis.

For the evaluation of H&E staining, the colitis scoring system described by Erben et al. was applied.[74] This scoring system includes histological features such as the level of inflammation, tissue architecture, and mucosal damage. These criteria were used to generate a score reflecting the severity of the colitis in each tissue sample. Additionally, the percentage of destroyed epithelium was calculated by comparing the damaged region to the total epithelial area in the individual samples, with destroyed epithelium defined as regions having a colitis score higher than 3. For Immunofluorescence staining, cells were manually counted using ImageJ Fiji. Manually counting the cells was crucial for accurately determining the number of cells expressing the specific markers, since there is no appropriate software. The results were visualized and analyzed using GraphPad Prism 10, a statistical analysis and graphing software. GraphPad Prism was used to generate bar graphs for easy comparison between different experimental groups. For statistical evaluation, ordinary one-way ANOVA was used to compare the means of multiple groups and determine statistically significant changes. Tukey's multiple comparisons test was applied to perform pairwise comparisons between groups. The significance level for all statistical tests was set at $p < 0.05$.

4. Results

4.1. Analgesic treatment: Colon

4.1.1. H&E staining

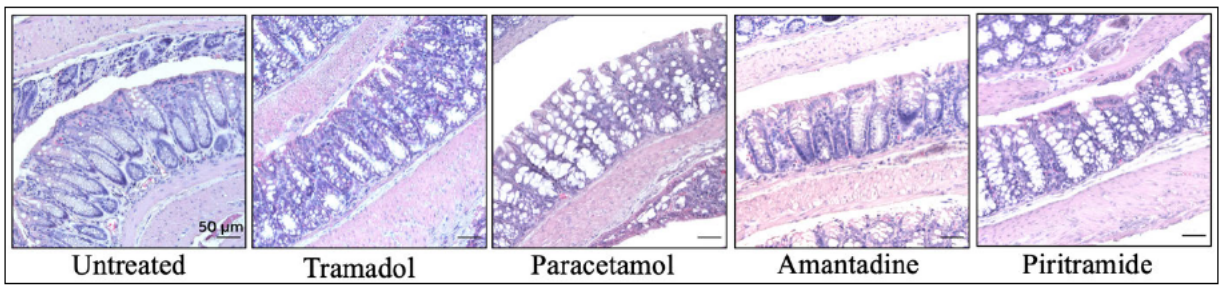

Figure 4. 1: H&E staining of colon without and after analgesic treatment

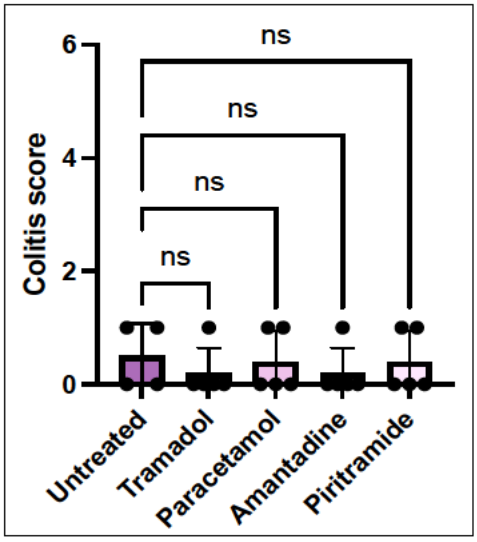

Figure 4. 2: Colitis score of colon without and after analgesic treatment
The colitis score was evaluated according to Erben et al. 2014, the significance in difference is shown above with ns = non-significant. One dot represents one mouse.

In Figure 4. 1 it can be seen that the use of analgesics led to either an increase in goblet cell size or number with paracetamol and piritramide showing the biggest changes and amantadine showing the least changes. However, the histomorphological scoring in Figure 4. 2 shows no significant change in inflammation, for either of the analgesics.

4.1.2. IF staining for immune response

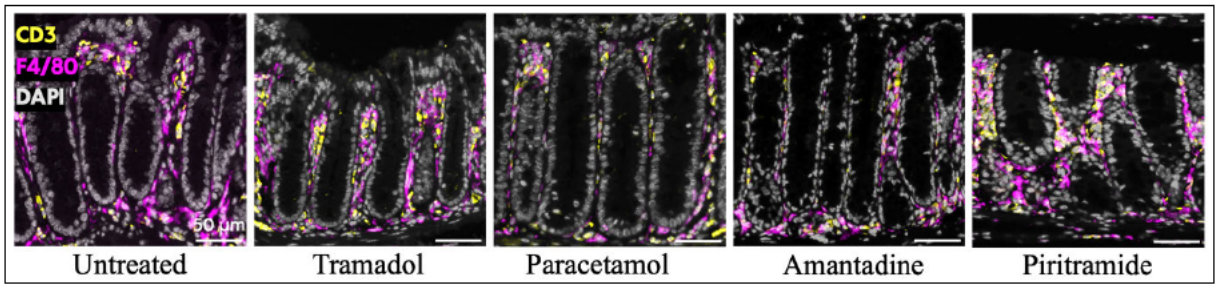

Figure 4. 3: Immunofluorescence staining for immune cells in colon without and after analgesic treatment
CD3 positive cells are shown in yellow, F4/80 positive cells in magenta and DAPI in grey in the colon without and after analgesic treatment.

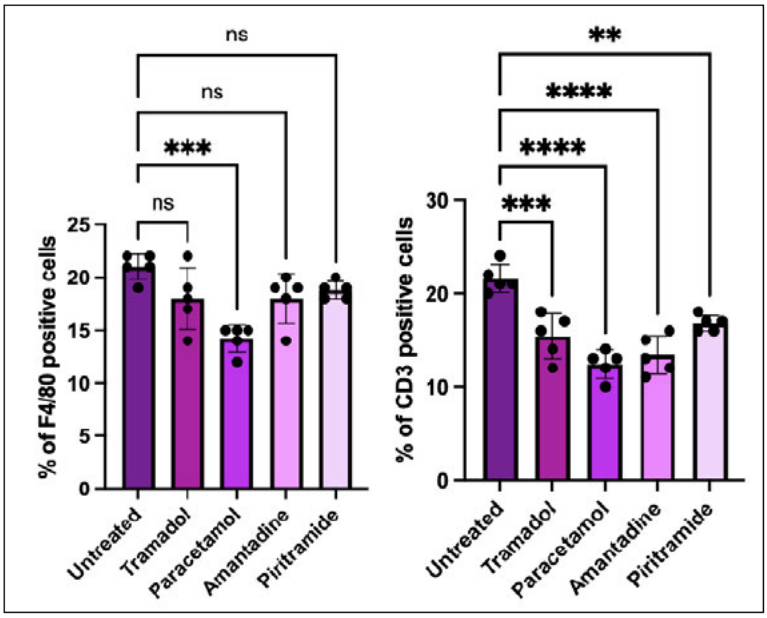

Figure 4. 4: Quantification of immune cells in colon without and after analgesic treatment
The total number of F4/80 (left) and CD3 (right) positive mucosal cells was quantitated, the significance in difference is shown above with ns = non-significant and more * indicating a higher significance. One dot represents one mouse.

A significant change in the mucosal macrophages, meaning F4/80 positive cells, was only detected in the paracetamol treated mice, however the use of all tested analgesics led to a reduction in the number of macrophages. On the other hand, the number of mucosal T-lymphocytes, shown by CD3, decreased with all four tested analgesics indicating an interference with the immune response.

4.1.3. IF staining for NF-κB response

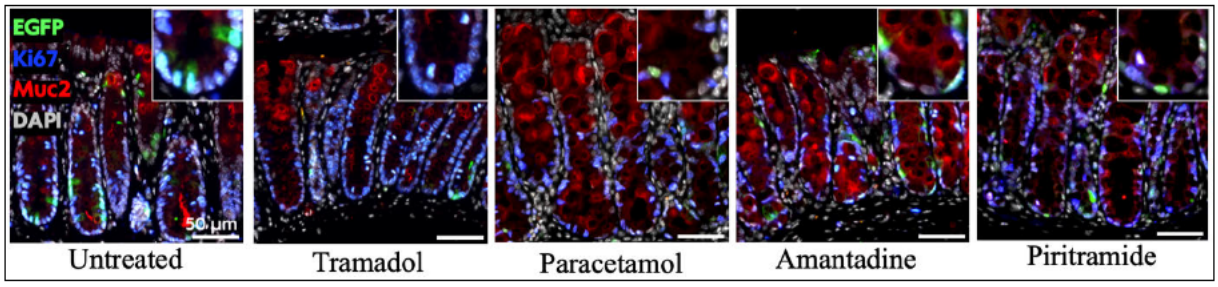

Figure 4. 5: Immunofluorescence staining for goblet, proliferating and NF-κB active cells in colon without and after analgesic treatment

EGFP positive cells showing NF-κB activity in green, Ki67 positive cells showing proliferation in blue, Muc2 positive cells indicating goblet cells in red and DAPI in grey in the colon without and after analgesic treatment.

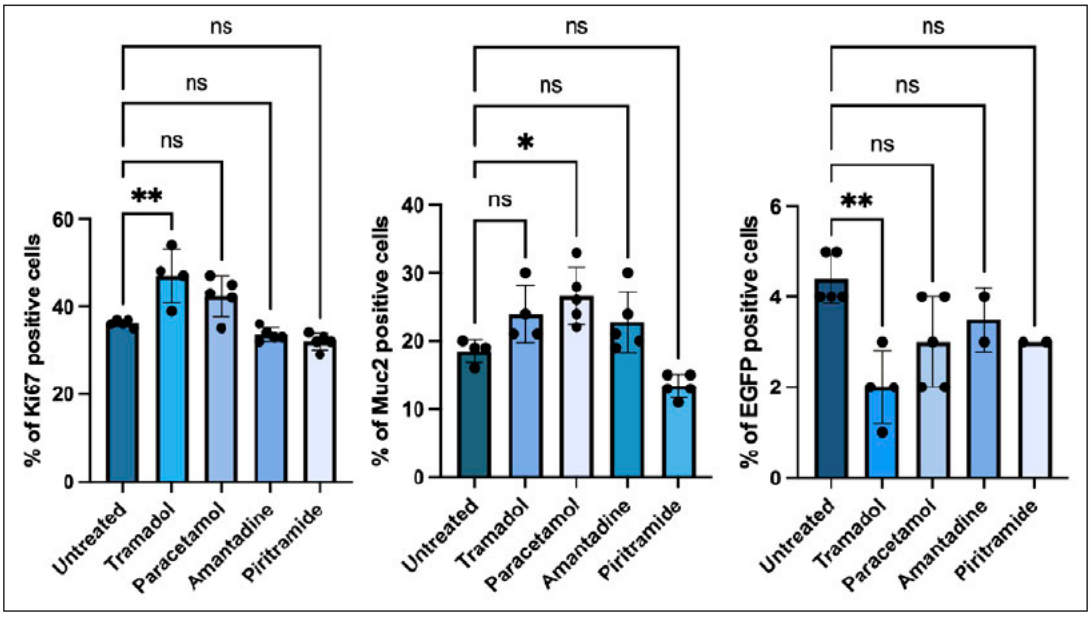

Figure 4. 6: Quantification of proliferating, goblet and NF-κB active cells in colon without and after analgesic treatment

The total number of Ki67 (left), Muc2 (middle) and EGFP (right) positive epithelial cells was quantitated, the significance in difference is shown above with ns = non-significant and more * indicating a higher significance. One dot represents one mouse.

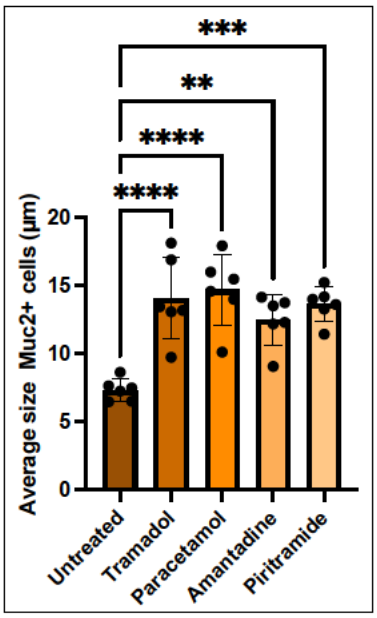

Figure 4. 7: Average size of Muc2 positive cells in colon without and after analgesic treatment
The average size of Muc2 positive cells, indicating goblet cells, in µm in colon samples. The significance in difference is shown above with more * indicating a higher significance. Each dot represents the average size of ten goblet cells from one mouse.

The H&E staining revealed prominent goblet cells; therefore, a Mucin 2 staining was done alongside with Ki67 to quantitate goblet and proliferating cells. There was only a significant change in the number of proliferating cells in the tramadol treated mice, the rest didn't show major differences. When looking at the number of goblet cells, there was only a significant difference in the paracetamol treated mice. However, the size of the goblet cells increased significantly in all of the treated mice, indicating an increased mucin production. Only in the tramadol treated mice a significant difference in the number of EGFP positive cells could be observed, showing a reduction in NF-κB activity.

4.2. Analgesic treatment: SII

4.2.1. H&E staining

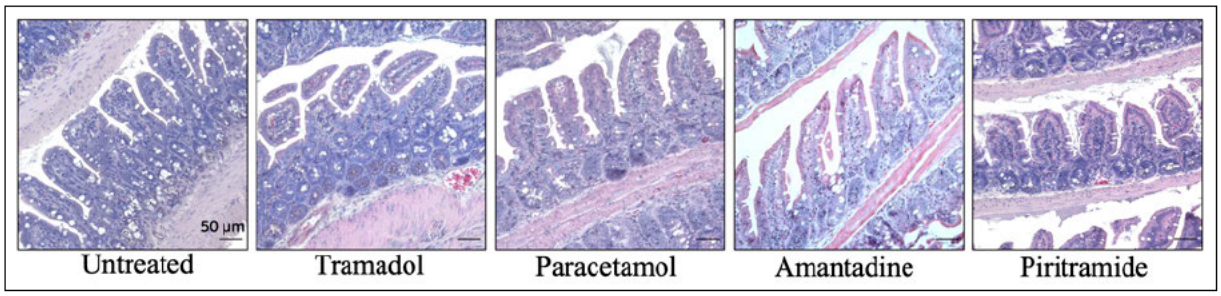

Figure 4. 8: H&E staining of SII without and after analgesic treatment

The H&E staining shows no visual difference between the untreated and treated ileum.

4.2.2. IF staining for immune response

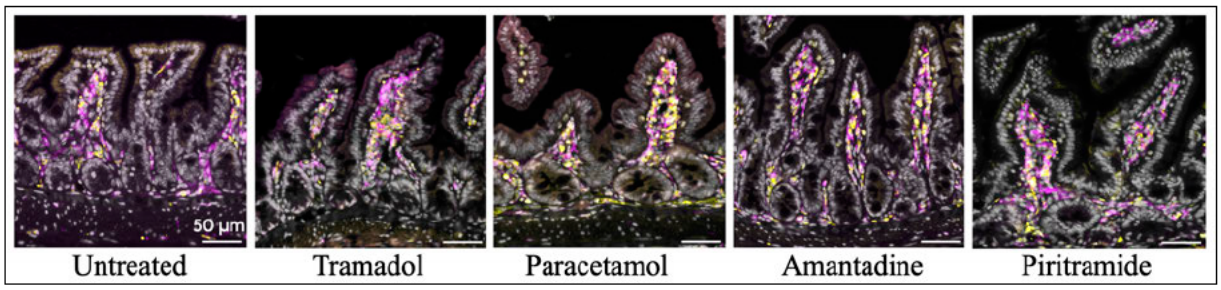

Figure 4. 9: Immunofluorescence staining for immune cells in SII without and after analgesic treatment
CD3 positive cells are shown in yellow, F4/80 positive cells in magenta and DAPI in grey in the ileum without and after analgesic treatment.

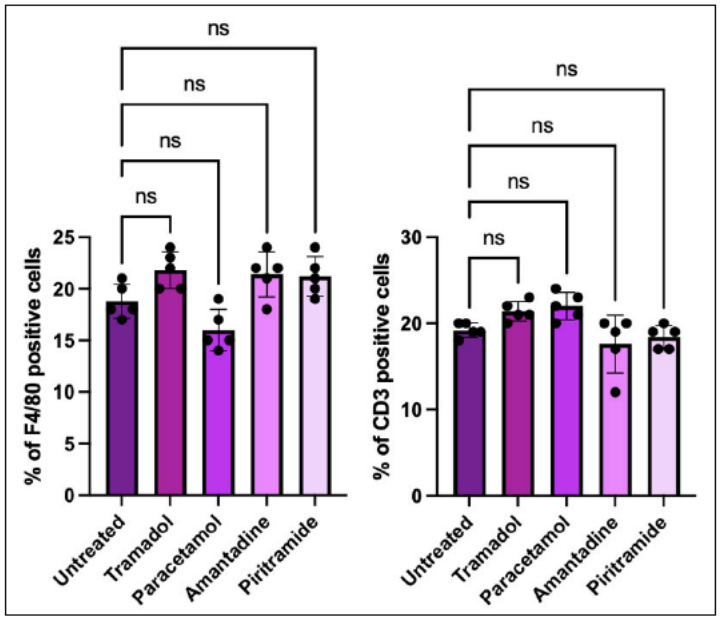

Figure 4. 10: Quantification of immune cells in SII without and after analgesic treatment
The total number of F4/80 (left) and CD3 (right) positive mucosal cells was quantitated in the ileum, the significance in difference is shown above with ns = non-significant. One dot represents one mouse.

Immunofluorescence staining reveals that none of the tested analgesics have a significant influence on the number of T-cells or macrophages, indicating no influence on the level of inflammation in the Ileum.

4.2.3. IF staining for NF-κB response

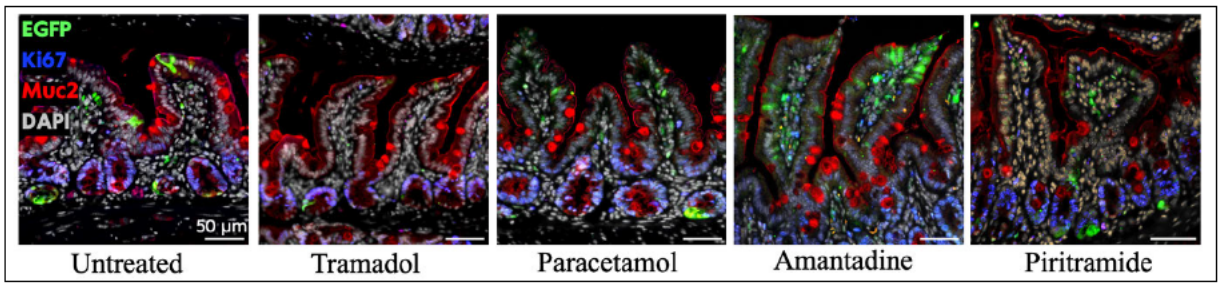

Figure 4. 11: Immunofluorescence staining for goblet, proliferating and NF-κB active cells in SII without and after analgesic treatment

EGFP positive cells showing NF-κB activity in green, Ki67 positive cells showing proliferation in blue, Muc2 positive cells indicating goblet cells in red and DAPI in grey in the ileum without and after analgesic treatment.

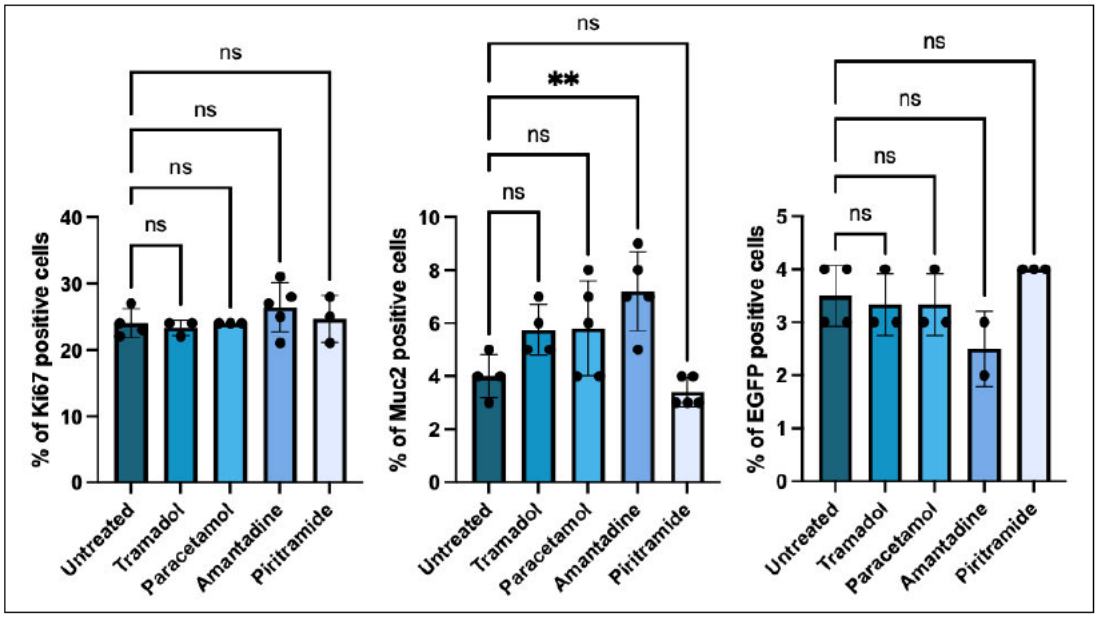

Figure 4. 12: Quantification of proliferating, goblet and NF-κB active cells in SII without and after analgesic treatment

The total number of Ki67 (left), Muc2 (middle) and EGFP (right) positive epithelial cells was quantitated, the significance in difference is shown above with ns = non-significant and more * indicating a higher significance. One dot represents one mouse.

None of the analgesics had a significant influence on the number of Ki67 and EGFP positive cells in the ileum. In addition to that, a change in the amount of goblet cells in the ileum can be observed with tramadol, paracetamol and amantadine, however only amantadine showed a significant influence.

4.3. DSS + amantadine treatment: Colon

4.3.1. H&E staining

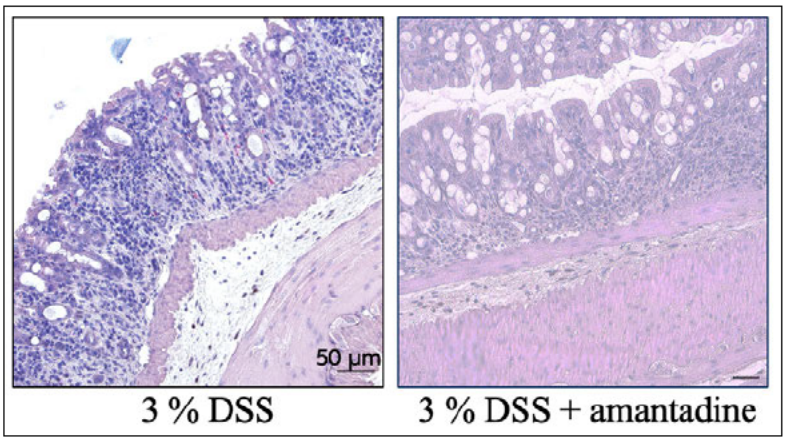

Figure 4. 13: H&E staining of colon after DSS or DSS + amantadine treatment
The mice were treated for 5 days with 3 % DSS or 3 % DSS and amantadine in the drinking water.

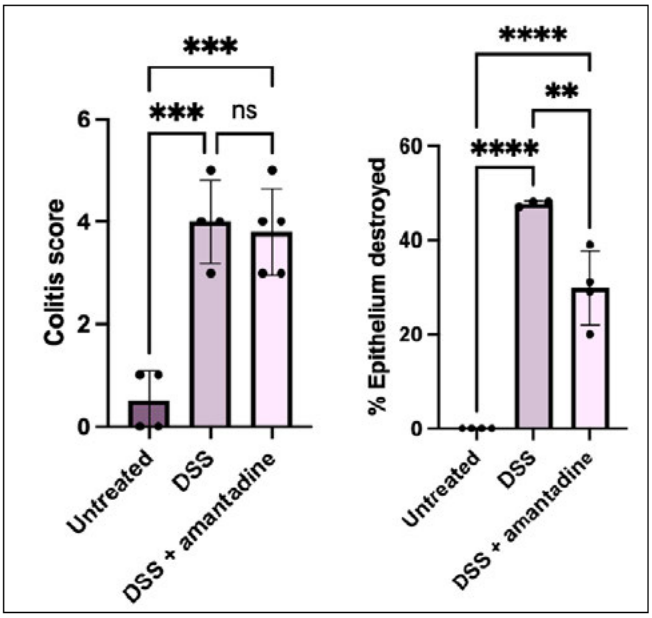

Figure 4. 14: Colitis score of colon after DSS or DSS + amantadine treatment and destruction of epithelium
The colitis score was evaluated according to Erben et al. 2014 and can be seen on the left. On the right the percentage of destroyed epithelium, meaning an area with the colitis score > 3 can be seen. The significance in difference is shown above with ns = non-significant and more * indicating a higher significance. One dot represents one mouse.

The use of DSS led to inflammation in the colon, shown by an increase in the colitis score, the additional use of amantadine in combination with DSS does not lead to a significant change in the colitis score. However, the amount of destroyed epithelium is significantly reduced when using additional amantadine, compared to DSS treatment alone.

4.3.2. IF staining for immune response

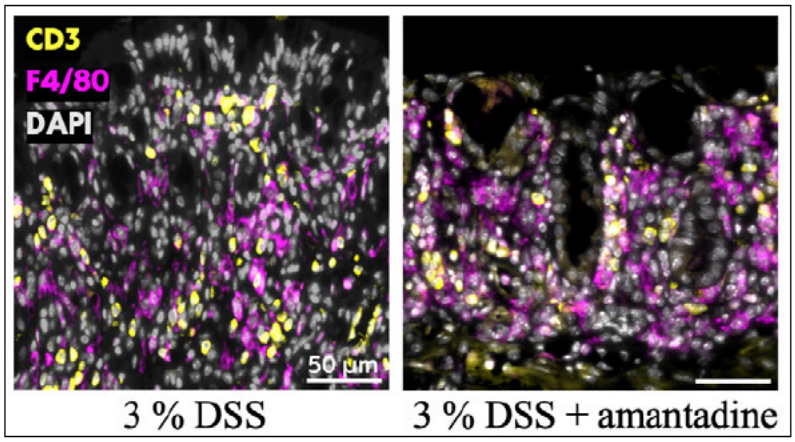

Figure 4. 15: Immunofluorescence staining for immune cells of colon after DSS or DSS + amantadine treatment
CD3 positive cells are shown in yellow, F4/80 positive cells are shown in magenta and DAPI in grey in the colon after 5 days of 3 % DSS or 3 % DSS + amantadine treatment.

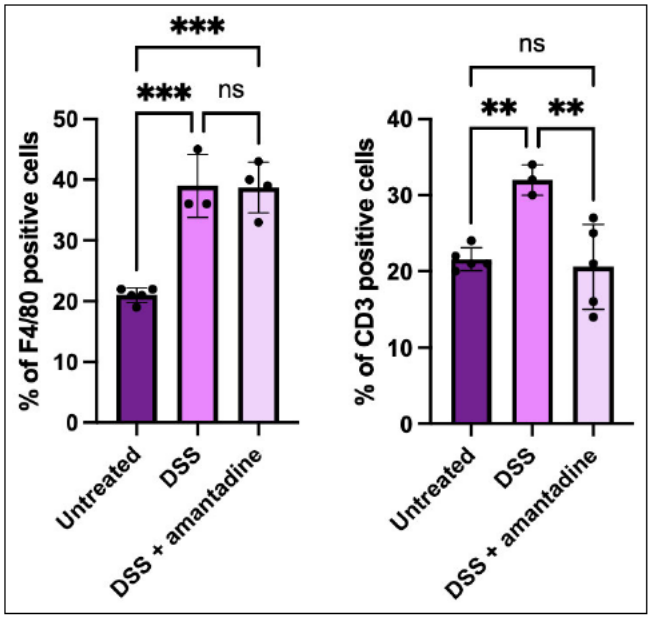

Figure 4. 16: Quantification of immune cells of colon after DSS or DSS + amantadine treatment
The total number of F4/80 (left) and CD3 (right) positive mucosal cells was quantitated, the significance in difference is shown above with ns = non-significant and more * indicating a higher significance. One dot represents one mouse.

In the colon, the number of macrophages showed a significant change following DSS treatment; however, no significant difference was observed when comparing DSS treatment alone to DSS treatment in combination with amantadine. But the addition of amantadine had a significant impact on the number of T-cells, as shown by the changed presence of CD3-positive cells. This indicates amantadine leading to a reduction on the level of inflammation of the colon.

4.3.3. IF staining for NF-κB response

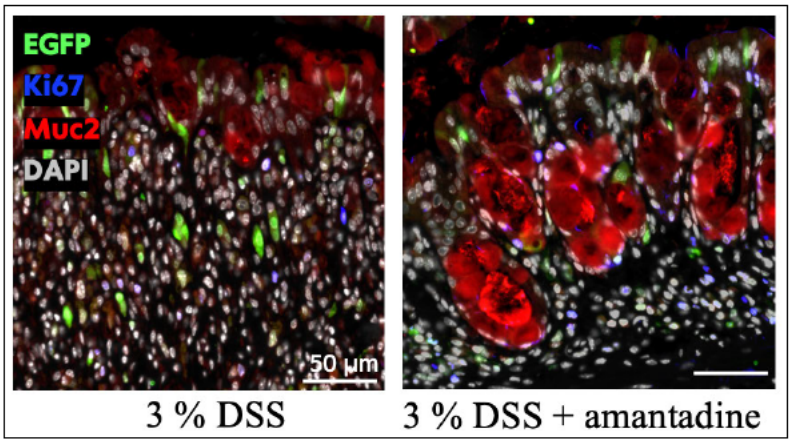

Figure 4. 17: Immunofluorescence staining for proliferating, goblet and NF-κB active cells of colon after DSS or DSS + amantadine treatment
EGFP positive cells showing NF-κB activity in green, Ki67 positive cells showing proliferation in blue, Muc2 positive cells indicating goblet cells in red and DAPI in grey in the colon after 5 days of 3 % DSS or 3 % DSS + amantadine treatment.

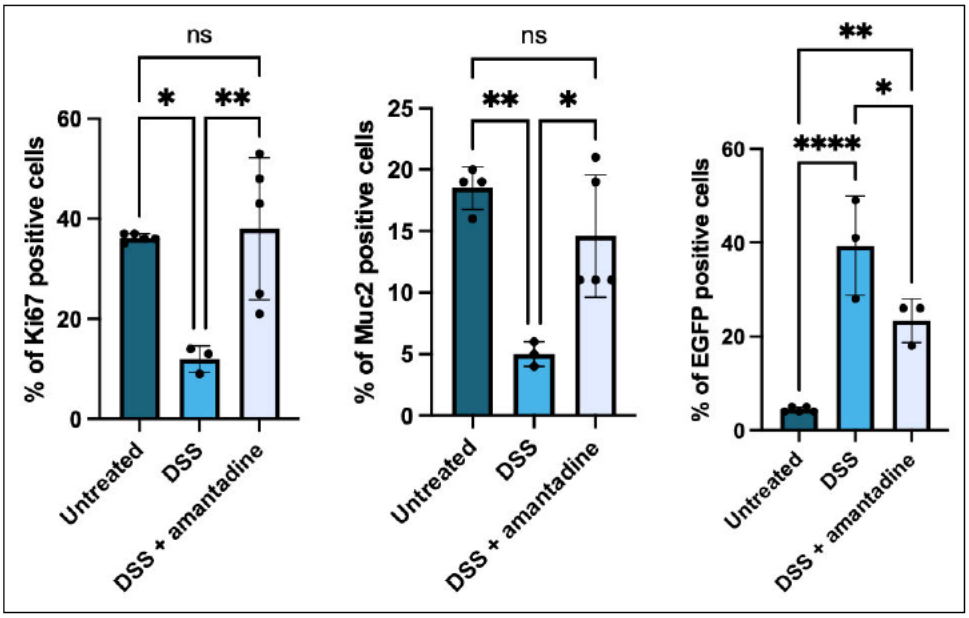

Figure 4. 18: Quantification of proliferating, goblet and NF-κB active cells of colon after DSS or DSS + amantadine treatment
The total number of Ki67 (left), Muc2 (middle) and EGFP (right) positive epithelial cells was quantitated, the significance in difference is shown above with ns = non-significant and more * indicating a higher significance. One dot represents one mouse.

The treatment of mice with DSS has a significant influence on the number of Ki67, Mucin 2 and EGFP positive cells in the colon. However, the use of amantadine in combination with DSS leads to a significant difference in the number of all three kinds compared to the use of DSS alone but only shows a significant difference in the number of EGFP positive cells when compared to the colon of untreated mice.

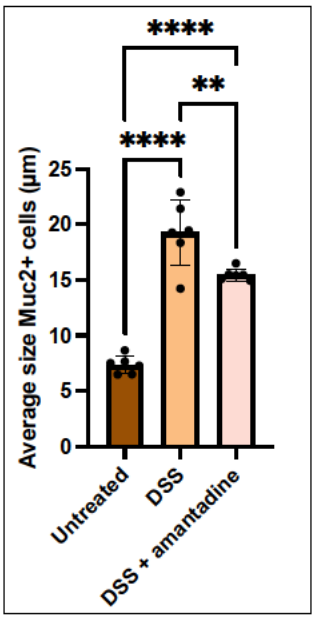

Figure 4. 19: Average size of Muc2 positive cells in colon after DSS or DSS + amantadine treatment
The average size of Muc2 positive cells, indicating goblet cells, in µm in the colon of mice after 5 days of 3 % DSS or 3 % DSS + amantadine treatment. The significance in difference is shown above with more * indicating a higher significance. Each dot represents the average size of ten goblet cells from one mouse.

The use of DSS led to a significant increase in goblet cell size, however, adding amantadine in combination with DSS led to a significant decrease in size compared to the goblet cell size after just DSS treatment alone indicating a reduction in mucin production.

4.4. DSS + amantadine treatment: SII

4.4.1. H&E staining

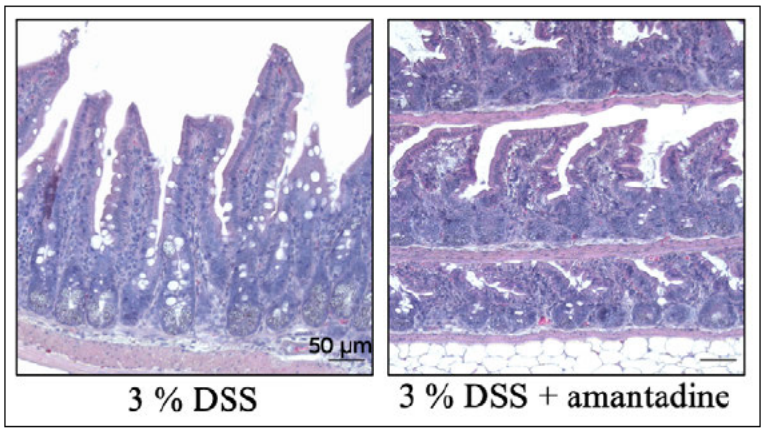

Figure 4. 20: H&E staining of SII after DSS or DSS + amantadine treatment
The mice were treated for 5 days with 3 % DSS or 3 % DSS and amantadine in the drinking water.

The H&E staining shows no visual difference between the ileum of DSS or DSS + amantadine treated mice.

4.4.2. IF staining for immune response

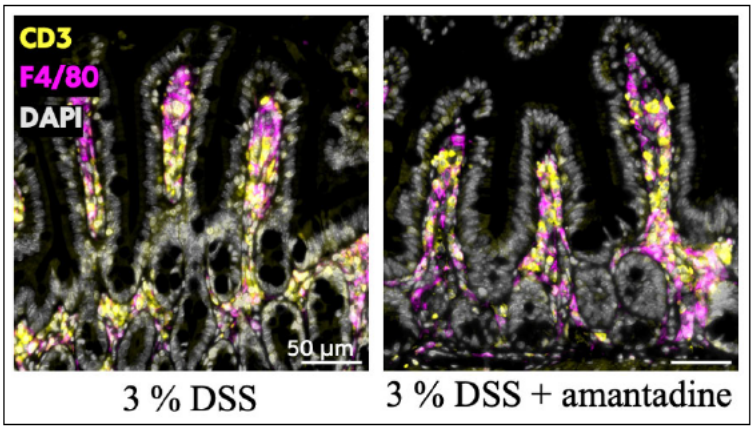

Figure 4. 21: Immunofluorescence staining for immune cells of SII after DSS or DSS + amantadine treatment
CD3 positive cells are shown in yellow, F4/80 positive cells are shown in magenta and DAPI in grey in the SII after 5 days of 3 % DSS or 3 % DSS + amantadine treatment.

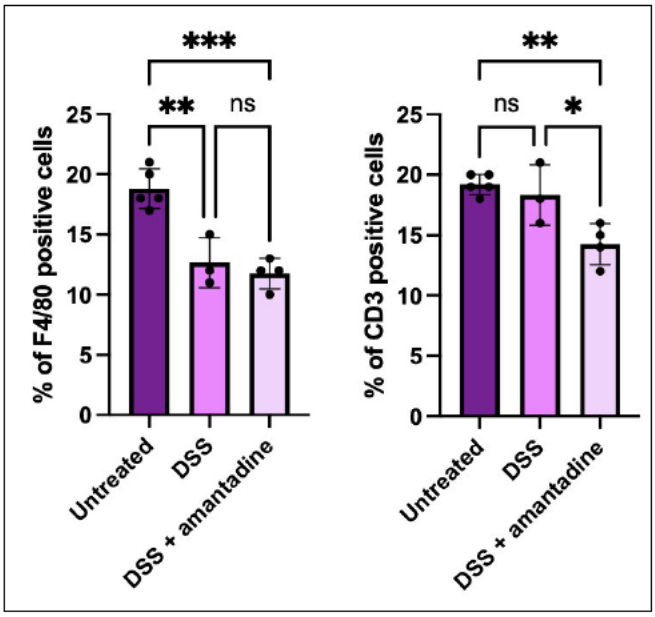

Figure 4. 22: Quantification of immune cells in SII after DSS or DSS + amantadine treatment
The total number of F4/80 (left) and CD3 (right) positive mucosal cells was quantitated, the significance in difference is shown above with ns = non-significant and more * indicating a higher significance. One dot represents one mouse.

A significant reduction in the number of F4/80 positive cells can be observed when comparing the ileum after DSS or DSS and amantadine treatment to the untreated ileum. However, not when comparing DSS and DSS with amantadine treated ileum. The addition of amantadine also leads to a significant reduction in T-cells, when compared to untreated and compared to after DSS treatment. Those however, do not show a significant difference in T-cell number.

4.4.3. IF staining for NF-κB response

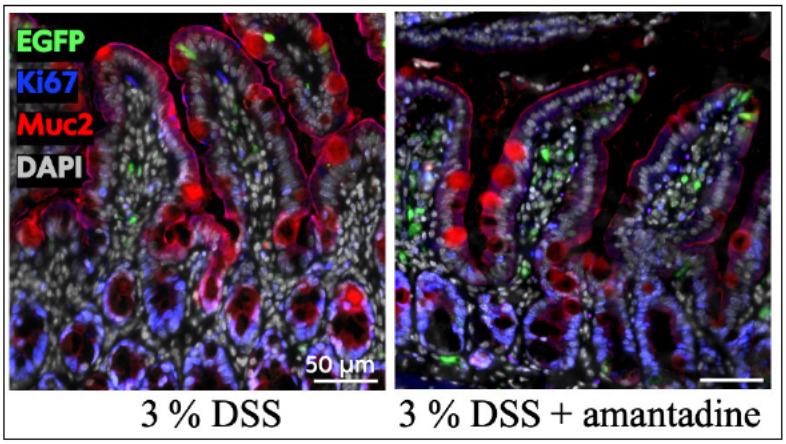

Figure 4. 23: : Immunofluorescence staining for proliferating, goblet and NF-κB active cells of SII after DSS or DSS + amantadine treatment
EGFP positive cells showing NF-κB activity in green, Ki67 positive cells showing proliferation in blue, Muc2 positive cells indicating goblet cells in red and DAPI in grey in the SII after DSS or DSS + amantadine treatment.

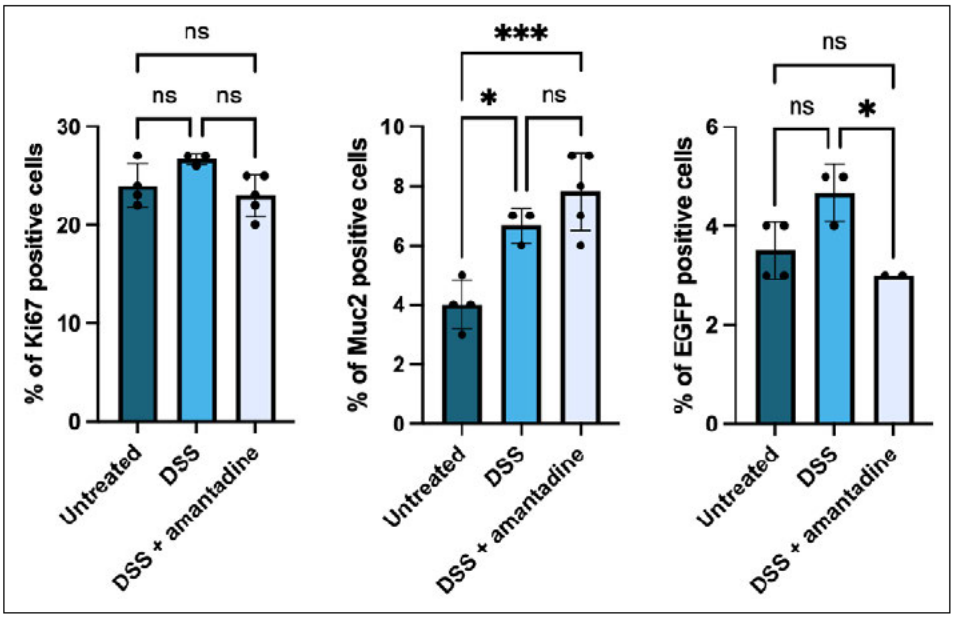

Figure 4. 24: Quantification of proliferating, goblet and NF-κB active cells of SII after DSS or DSS + amantadine treatment
The total number of Ki67 (left), Muc2 (middle) and EGFP (right) positive epithelial cells was quantitated, the significance in difference is shown above with ns = non-significant and more * indicating a higher significance. One dot represents one mouse.

Using amantadine with DSS does not have a significant influence on the number of Ki67 or Mucin 2 positive cells compared to DSS treatment alone. However, the number of cells with activated NF-κB is significantly reduced after the additional use of amantadine, compared to when using just DSS.

5. Discussion

The DSS induced colitis model is the most commonly employed approach for modelling UC.[19] However, the symptoms caused by DSS ingestion, including bloody diarrhea, can cause abdominal discomfort up to painful cramps.[28] In this study, the applicability of analgesics without causing an interference with research targets, was investigated. The basis for this was the identification of the most promising candidates using a deep learning based search with the program PEDL+, which identified amantadine and piritramide. Additionally, tramadol and paracetamol were used as positive controls, due to their recommended application for this model by LAGeSo. Those four analgesics were then validated and their applicability analyzed in a murine model before the most promising one was tested in the DSS colitis model.

5.1. Influence of analgesics on the colon

In the first part of this study, mice were treated with the analgesics on their own, without the induction of UC. The H&E staining of colon revealed no visible change in the colitis score. However, it was observed that there was a change in either the number or size of goblet cells. This could mainly be detected in paracetamol and piritramide treated mice, whereas amantadine treatment led to the least visually observable changes in goblet cells. The IF staining for the immune response showed that all tested analgesics led to a reduction of immune cells, showing that all of them interfere with the immune response. In addition to that, further IF staining confirmed the findings from the H&E staining. While the overall number of goblet cells only significantly increased in the colon of paracetamol treated mice, the average diameter of goblet cells increased significantly after treatment with all the tested drugs. This may be a compensatory mechanism to enhance the epithelial barrier by thickening the mucosal layer in response to the external agents. While increased Muc2 production can help strengthen the mucosal barrier and potentially prevent inflammation, this effect works against the primary objective of the DSS induced colitis model. Here, the induction and maintenance of inflammation in the colon is essential for accurately studying the disease mechanisms and evaluating treatment options. An enhanced barrier function may reduce the severity of inflammation, making it difficult to assess the full inflammatory response typical of UC. From the tested analgesics, the colon of amantadine-treated mice showed goblet cell numbers and sizes most similar to the untreated control group. This suggests that amantadine had the least

impact on mucin production and, therefore, may be the most promising drug for use in the colitis models. Additionally, paracetamol and tramadol treatment led to the biggest goblet cell changes, supporting the finding that the PEDL+ selected analgesics are appropriately chosen. When examining changes in cell proliferation, a similar pattern shows. Tramadol and paracetamol treatment led to an increase in the number of Ki67 positive cells compared to untreated mice, indicating enhanced cellular proliferation. In contrast, amantadine and piritramide treatment resulted in values most similar to those observed in untreated mice.

Looking at the results from the EGFP staining, only tramadol treatment resulted in a significant reduction, indicating a decrease in NF-κB activity. However, all tested analgesics appeared to reduce NF-κB activity to some extent. Notably, paracetamol showed a large standard deviation, suggesting variability in its effect. Again, amantadine displayed results most similar to the untreated mice.

Overall, the PEDL+-selected analgesics showed less differences in their effects on NF-κB activity, cell proliferation, goblet cell characteristics and immune cells in comparison to tramadol and paracetamol. From amantadine and piritramide, amantadine emerged as the most promising candidate due to its similarity to the untreated group, based on the investigated parameters. Therefore, it was selected for further validation in the DSS-induced UC model.

5.2. Influence of analgesics on the SII

In this study, the primary focus was on the colon, as it is the main site affected by UC and the part where inflammation predominantly occurs. However, in order to gain more understanding of the systemic effects of the tested analgesics, the SII was also analyzed. The H&E staining of the ileum revealed no visible differences between the untreated and analgesic treated groups, suggesting no major histological alterations. Immunofluorescence staining further supported this observation, as none of the tested analgesics significantly influenced the number of T-cells or macrophages in the ileum. This indicates that the analgesics did not induce or suppress inflammation in this part of the small intestine. Similarly, no significant changes were observed in the number of Ki67 positive proliferating cells or EGFP positive cells, suggesting that NF-κB activity and epithelial cell turnover remained unaffected by analgesic treatment in the ileum. Interestingly, while tramadol, paracetamol, and amantadine all led to changes in the number of goblet cells, only amantadine showed a significant change. This suggests that amantadine may

uniquely impact mucin production or goblet cell dynamics and can have a direct influence on mucin-related pathways in the ileum. But the relevance of this finding in the context of UC remains uncertain, especially due to the lack of inflammatory or proliferative changes in the ileum. Overall, these findings show that, unlike the colon, the SII remains relatively unaffected by the tested analgesics.

The immune environment differs greatly between the ileum and the colon.[75] This may be an explanation as to why the tested analgesics led to significant changes in the colon but not in the small intestine. The colon is exposed to a much denser and more diverse microbial population than the ileum, leading to a higher baseline immunity. The constant exposure to these antigens may make the immune system in the colon more reactive to external stimuli, like analgesics, and can be a cause for the observed differences in immune cells, goblet cells and NF-κB activity.

5.3. Amantadine in the colitis model: colon

The results of H&E staining reveal, that the treatment of mice with DSS leads to an inflammation of the colon, evidenced by the significant increase in the colitis score. The addition of amantadine did not lead to a further significant change in the colitis score. However, the amount of destroyed epithelium was significantly reduced in the amantadine-treated group compared to DSS treatment alone. This indicates a potential protective effect of amantadine on epithelial integrity, which may contribute to maintaining the physical barrier of the epithelial layer despite ongoing inflammation. This can be explained by the results obtained from the IF staining, where amantadine treatment alone led to an increase in mucin production, strengthening the mucinous barrier.

When looking at changes of the immune cells, the DSS treatment led to a significant increase in macrophage numbers, the addition of amantadine did not further significantly influence those. This again aligns with previous findings, where amantadine treatment alone also did not significantly influence macrophage numbers, suggesting that amantadine does not directly affect macrophage recruitment. In contrast to that, the addition of amantadine has a significant effect on the number of T-cells. In both, the colitis model and when administered alone, T-cell numbers significantly decreased after amantadine administration. This difference is especially important when comparing DSS treatment alone to in combination with amantadine. This

indicates immunomodulatory properties of amantadine and presents a challenge when using this model to study the immune response in ulcerative colitis. Since T-cells play a central role in driving inflammation and tissue damage in UC, any external influence on their numbers could impact the natural progression of inflammation, working against the purpose of the colitis model.

The analysis of epithelial cell staining revealed that the addition of amantadine leads to a significant increase of the number of Ki67 positive proliferating cells and Muc2 positive goblet cells, as well as a significant reduction of EGFP-positive cells, indicative of NF-κB activity, when compared to DSS treatment alone. This shows that amantadine has a strong effect on the behavior of epithelial cells. Regarding the size of goblet cells, DSS treatment alone led to a significant increase, showing an upregulation of mucin production, however the addition of amantadine reversed this effect, leading to a significant decrease in goblet cell size compared to DSS alone, but still an increase compared to untreated. Increased mucin production is a protective measure against inflammation, however it can also be seen as a state of epithelia stress. The ability of amantadine to reduce goblet cell size may indicate a return to a less inflamed and more homeostatic epithelial environment, which aligns with the numbers of proliferating, goblet and T-cells being similar to those of the untreated group.

Looking at NF-κB activity and comparing the colon of DSS + amantadine treated mice to the untreated control group only the number of EGFP-positive cells remained significantly different. This suggests that while amantadine modulates DSS induced changes, it does not fully restore epithelial homeostasis to prior to the treatment. The reduction in EGFP-positive cells is particularly interesting, as NF-κB activity is one of the primary targets of investigation in this study. Any interference with NF-κB signaling can strongly affect the results, as it may obscure the actual relationship between inflammation and epithelial responses. Since NF-κB is a central regulator of immune responses, including the activation of inflammatory pathways, alterations in its activity caused by amantadine could bias findings regarding the mechanisms driving UC. This interference complicates and may even prohibit the assessment of inflammation and of the efficacy of potential therapeutic targets, making it difficult to differentiate between the influence of amantadine and the investigated disease. This aligns with the observed decrease in T-cell numbers, indicating that amantadine may suppress NF-κB signaling, contributing to its anti-inflammatory effects.

Overall, the addition of amantadine has a multifaceted effect on the colon in the DSS induced UC model. While it does not reduce the overall colitis score, it appears to protect epithelial integrity and decreases key markers of inflammation, including T-cell infiltration and NF-κB activity. The normalization of goblet cell number and size supports the idea that amantadine may work against the inflammation caused by DSS. However, this is against the goal of the DSS induced UC model which aims to induce and study chronic inflammation and tissue damage resembling the disease in humans.

5.4. Amantadine in the colitis model: SII

The H&E staining revealed no visible morphological differences between the ileum of DSS-treated mice and those receiving DSS in combination with amantadine, suggesting that amantadine does not induce major structural changes in the small intestine. The IF staining showed a significant reduction in macrophage numbers when comparing the ileum of both, the DSS and the DSS + amantadine treated to untreated mice. However, no significant difference was detected between the DSS and the DSS + amantadine group. This indicates that while DSS itself reduces macrophage numbers in the SII, amantadine does not further increase this effect. The reduction in macrophages may suggest a diminished inflammatory environment or disrupted immune signaling based on their role in promoting homeostasis and coordinating immune responses. A big differences however could be seen in the significant reduction of T-cells, when comparing DSS + amantadine to untreated and only DSS treated. This aligns with the observations made in the colon and suggests that amantadine influences T-cell recruitment or retention in the intestinal mucosa. This is particularly important in the context of a colitis model, where a strong immune response is a key feature of disease pathology. Therefore, by reducing T-cell numbers, amantadine may decrease inflammation and alter the overall immune dynamics, potentially interfering with the intended inflammatory profile of the DSS model.

As previously described, BWI is a condition observed in UC patients, where the colonic contents backwash into the small intestine and cause inflammation and nutrient malabsorption. The oral administration of DSS mainly affects the colon and so far, the DSS induced colitis model has not been studied for its use to model BWI. In this study, the H&E staining revealed no major histological changes. IF staining shows a reduction in macrophage and T-cell numbers, indicating that DSS exposure does have an effect on immune cells beyond the colon, however to a lesser extent.

Interestingly, amantadine did not significantly affect the number of proliferating or goblet cells compared to DSS treatment alone. This suggests that, unlike in the colon, amantadine does not significantly influence epithelial turnover or mucin production in the SII. This difference could be due to the inherently lower inflammatory baseline in the small intestine compared to the colon, making it less susceptible to external modulators like amantadine. NF-κB activity, based on the number of EGFP-positive cells, was significantly reduced in the ileum following amantadine administration. This reduction aligns with findings in the colon.

Overall, these findings indicate that amantadine exerts similar immunomodulatory effects in the Ileum as observed in the colon, particularly in reducing T-cell numbers and suppressing NF-κB activity. While these effects may reflect a potential protective or anti-inflammatory action, they also compromise the integrity of the DSS colitis, therefore limiting the utility of the UC model in accurately reflecting the immune-mediated pathology of the disease.

6. Conclusion

The aim of this study was the identification of the best fitting analgesic to be used in the DSS induced ulcerative colitis model. The basis for this research was the pre-selection of the most promising drug candidates using the deep learning based program PEDL+, which identified amantadine and piritramide. Furthermore, paracetamol and tramadol were selected as positive controls. The focus were the effects on intestinal inflammation and NF-κB activity.

In the healthy colon, all tested analgesics led to increased goblet cell size, suggesting a general enhancement of mucin production. However, amantadine-treated mice showed the most similar goblet cell number and size as well as number of EGFP positive cells to untreated controls, making it the most promising candidate for minimizing interference in colitis studies. In contrast, tramadol induced significant changes in both proliferating and EGFP-positive cell numbers, while paracetamol treatment led to significant changes in macrophage and goblet cell numbers, highlighting their stronger modulatory effects on NF-κB activity as well as epithelial and immune cells. These results demonstrate that the commonly used analgesics in murine research can introduce significant biases in colitis studies. However, this also highlights the effectiveness of the PEDL+ based pre-selection method, as the analgesics identified through this approach produced overall more promising results than paracetamol and tramadol.

In the DSS colitis model, amantadine did not significantly alter the overall colitis score but appeared to protect epithelial integrity, reduce T-cell infiltration, and suppress NF-κB activity in the colon. This shows that amantadine interferes with some of the research targets crucial for studying UC pathogenesis. A similar trend was observed in the small intestine, where amantadine treatment resulted in a reduction of T-cells and NF-κB activity, despite no major structural alterations in the ileum. These systemic effects highlight the need for careful consideration when selecting analgesics for their use in the DSS colitis model, as they can significantly influence immune cells and NF-κB activity. Even the most promising candidate, amantadine, is not ideal for all research targets. While it may be suitable for certain investigations, its effects could interfere with studies focusing on NF-κB activity and immune responses. From the perspective of the 3R principles, it would be more ethical and efficient to avoid analgesics when possible, allowing the collected biopsies to be utilized for a broader range of research purposes. The alternative, which would be to use an analgesic and limit the applicability of the samples, could lead to the need for additional animal experiments, for instance for studies where the analgesic influences the research target. Therefore, careful

consideration should be given to whether the use of analgesics is necessary in each specific experimental setup to minimize the overall number of animals required while ensuring scientific validity.

7. Outlook

While this study provides valuable insights into the effects of different analgesics in the DSS-induced colitis model, several aspects require further investigation to ensure the validity and accuracy of the findings. One critical point is the necessity of CDH1 and EGFP co-staining to determine whether EGFP-positive cells are indeed intestinal epithelial cells or if NF-κB activation occurs in other cell populations as well. This distinction is crucial, as a misinterpretation of EGFP expression patterns could impact the conclusions drawn about NF-κB activity in the intestinal epithelium. If non-epithelial cells also contribute significantly to the EGFP signal, some of the current findings may require reassessment.

Additionally, further validation of amantadine and piritramide treatment is necessary. Given the limited number of EGFP-positive mice treated with these analgesics, increasing the sample size would strengthen the reliability of the observed effects and ensure that the observations made in this study remain valid under harsher statistical settings. Expanding these experiments would provide a more robust basis for evaluating the suitability of these analgesics in the DSS model.

Another important consideration is whether the effects of DSS and the tested analgesics might change under different treatment durations or within a DSS recovery model. If recovery of inflammation or tissue regeneration alters the impact of analgesic treatment over time, additional studies examining longer recovery phases or shorter treatment periods could provide a better understanding of the effects of analgesic use. Investigating these variables would help determine whether the observed effects are consistent across different experimental conditions or if they are specific to the time frame used in this study. Furthermore, another important aspect is the analysis of gene expression in the colon samples using qPCR. This could provide insight into how the tested analgesics influence key inflammatory and epithelial markers at the transcriptional level, including NF-κB signaling, mucin production, epithelial integrity, and immune cell activity.

Ultimately, refining the characterization of EGFP-positive cells, increasing the number of animals in key experimental groups, and exploring different treatment durations will enhance the interpretability of the results. These steps will be advantageous in determining whether an analgesic like amantadine could be reliably used, ensuring that future preclinical studies maintain both ethical considerations and scientific accuracy.

Affidavit / Declaration of Authorship

I, Lisa Drees, hereby declare that this master thesis is my own original work and that I wrote it independently and without external assistance. All passages taken directly or indirectly from other sources have been properly cited and referenced. This thesis has not been submitted, in whole or in part, for any other academic degree or examination at any institution.

Hamburg, 27.02.2025 

Acknowledgements

First and foremost, I would like to express my gratitude to my supervisor, Marina Kolesnichenko, for her support and encouragement throughout this project and allowing me to participate in her groups research.

I am also deeply grateful to the entire AG Kolesnichenko, Antony, Tim and Luisa, for introducing me to everything and helping me whenever needed, as well as making the time in the lab so fun and unforgettable for me.

Furthermore, a big thank you to my university supervisor, Julien Béthune, for supporting me in both my studies and in this thesis.

A special thank you goes to my father and my sisters for supporting me throughout everything, especially their emotional support and encouragement throughout my whole academic journey. And an extra thanks to my father for making it possible for me to pursue my studies!

Lastly, I would like to thank Kai, for his patience, for proofreading my thesis, and for always being there to support me.

8. Literature

1. Ericsson, A. C., Crim, M. J. & Franklin, C. L. A brief history of animal modeling. Mo Med 110, 201–205 (2013).
2. Sabin, A. B. Oral Poliovirus Vaccine: History of Its Development and Prospects for Eradication of Poliomyelitis. JAMA 194, 872 (1965).
3. National Research Council (US) and Institute of Medicine (US) Committee. Use of Laboratory Animals in Biomedical and Behavioral Research. (National Academies Press (US), Washington (DC), 1988).
4. King, A. J. The use of animal models in diabetes research. British J Pharmacology 166, 877–894 (2012).
5. Andersen, M. L. & Winter, L. M. F. Animal models in biological and biomedical research - experimental and ethical concerns. An. Acad. Bras. Ciênc. 91, e20170238 (2019).
6. Bundesinstitut für Risikobewertung. Verwendung von Versuchstieren Im Berichtsjahr 2023. https://www.bf3r.de/de/verwendung_von_versuchstieren_im_berichtsjahr_2023-318066.html (2024).
7. Rinwa, P., Eriksson, M., Cotgreave, I. & Bäckberg, M. 3R-Refinement principles: elevating rodent well-being and research quality. Lab Anim Res 40, 11 (2024).
8. Russell, W. M. S. & Burch, R. L. The Principles of Humane Experimental Technique. (Universities Federation for Animal Welfare, Potters Bar, Herts, 1992).
9. Petetta, F. & Ciccocioppo, R. Public perception of laboratory animal testing: Historical, philosophical, and ethical view. Addict Biol 26, e12991 (2021).
10. Europäisches Parlament und Rat der EU. RICHTLINIE 2010/63/EU DES EUROPÄISCHEN PARLAMENTS UND DES RATES. (2010).
11. Joshi, A., Soni, A. & Acharya, S. In vitro models and ex vivo systems used in inflammatory bowel disease. In Vitro Model 1, 213–227 (2022).
12. Macedo, M. H., Dias Neto, M., Pastrana, L., Gonçalves, C. & Xavier, M. Recent Advances in Cell-Based In Vitro Models to Recreate Human Intestinal Inflammation. Advanced Science 10, 2301391 (2023).
13. Khor, B., Gardet, A. & Xavier, R. J. Genetics and pathogenesis of inflammatory bowel disease. Nature 474, 307–317 (2011).
14. Stokkers, P. C. F. & Hommes, D. W. New cytokine therapeutics for inflammatory bowel disease. Cytokine 28, 167–173 (2004).
15. Abraham, C. & Cho, J. H. Inflammatory bowel disease. N Engl J Med 361, 2066–2078 (2009).
16. Ordás, I., Eckmann, L., Talamini, M., Baumgart, D. C. & Sandborn, W. J. Ulcerative colitis. Lancet 380, 1606–1619 (2012).
17. Kucharzik, T., Koletzko, S., Kannengiesser, K. & Dignass, A. Ulcerative Colitis-Diagnostic and Therapeutic Algorithms. Dtsch Arztebl Int 117, 564–574 (2020).
18. Kobayashi, T. et al. Ulcerative colitis. Nat Rev Dis Primers 6, 74 (2020).
19. Katsandegwaza, B., Horsnell, W. & Smith, K. Inflammatory Bowel Disease: A Review of Pre-Clinical Murine Models of Human Disease. Int J Mol Sci 23, 9344 (2022).
20. Erden, A. et al. Backwash ileitis in ulcerative colitis: Are there MR enterographic features that distinguish it from Crohn disease? Eur J Radiol 110, 212–218 (2019).
21. Chassaing, B. et al. Dietary emulsifiers impact the mouse gut microbiota promoting colitis and metabolic syndrome. Nature 519, 92–96 (2015).
22. Porter, R. J., Kalla, R. & Ho, G.-T. Ulcerative colitis: Recent advances in the understanding of disease pathogenesis. F1000Res 9, F1000 Faculty Rev-294 (2020).
23. Tatiya-aphiradee, N., Chatuphonprasert, W. & Jarukamjorn, K. Immune response and inflammatory pathway of ulcerative colitis. Journal of Basic and Clinical Physiology and Pharmacology 30, 1–10 (2018).

24. Fedi, A. et al. In vitro models replicating the human intestinal epithelium for absorption and metabolism studies: A systematic review. J Control Release 335, 247–268 (2021).
25. Roh, T. T., Chen, Y., Rudolph, S., Gee, M. & Kaplan, D. L. InVitro Models of Intestine Innate Immunity. Trends Biotechnol 39, 274–285 (2021).
26. Dieleman, L. A. et al. Chronic experimental colitis induced by dextran sulphate sodium (DSS) is characterized by Th1 and Th2 cytokines. Clin Exp Immunol 114, 385–391 (1998).
27. Mizoguchi, A. Animal models of inflammatory bowel disease. Prog Mol Biol Transl Sci 105, 263–320 (2012).
28. Wirtz, S., Neufert, C., Weigmann, B. & Neurath, M. F. Chemically induced mouse models of intestinal inflammation. Nat Protoc 2, 541–546 (2007).
29. Perše, M. & Cerar, A. Dextran sodium sulphate colitis mouse model: traps and tricks. J Biomed Biotechnol 2012, 718617 (2012).
30. Dieleman, L. A. et al. Dextran sulfate sodium-induced colitis occurs in severe combined immunodeficient mice. Gastroenterology 107, 1643–1652 (1994).
31. Vezza, T. et al. Minocycline Prevents the Development of Key Features of Inflammation and Pain in DSS-induced Colitis in Mice. J Pain 24, 304–319 (2023).
32. Dolcet, X., Llobet, D., Pallares, J. & Matias-Guiu, X. NF-kB in development and progression of human cancer. Virchows Arch 446, 475–482 (2005).
33. Lin, Y., Bai, L., Chen, W. & Xu, S. The NF-kappaB activation pathways, emerging molecular targets for cancer prevention and therapy. Expert Opin Ther Targets 14, 45–55 (2010).
34. Zhang, C., Lillie, R., Cotter, J. & Vaughan, D. Lysozyme purification from tobacco extract by polyelectrolyte precipitation. Journal of Chromatography A 1069, 107–112 (2005).
35. Wang, L. et al. IL-6 induces NF-kappa B activation in the intestinal epithelia. J Immunol 171, 3194–3201 (2003).
36. Nenci, A. et al. Epithelial NEMO links innate immunity to chronic intestinal inflammation. Nature 446, 557–561 (2007).
37. Laurindo, L. F. et al. Phytochemicals and Regulation of NF-kB in Inflammatory Bowel Diseases: An Overview of In Vitro and In Vivo Effects. Metabolites 13, 96 (2023).
38. Peng, C., Ouyang, Y., Lu, N. & Li, N. The NF-κB Signaling Pathway, the Microbiota, and Gastrointestinal Tumorigenesis: Recent Advances. Front Immunol 11, 1387 (2020).
39. Messeri, L. & Crockett, M. J. Artificial intelligence and illusions of understanding in scientific research. Nature 627, 49–58 (2024).
40. Deiana, A. M. et al. Applications and Techniques for Fast Machine Learning in Science. Front Big Data 5, 787421 (2022).
41. PubMed, National Institutes of Health (NIH). PubMed Overview. https://pubmed.ncbi.nlm.nih.gov/about (2023).
42. Jin, Q., Leaman, R. & Lu, Z. PubMed and beyond: biomedical literature search in the age of artificial intelligence. EBioMedicine 100, 104988 (2024).
43. Beltagy, I., Lo, K. & Cohan, A. SciBERT: A Pretrained Language Model for Scientific Text. (2019) doi:10.48550/ARXIV.1903.10676.
44. Weber, L., Thobe, K., Migueles Lozano, O. A., Wolf, J. & Leser, U. PEDL: extracting protein-protein associations using deep language models and distant supervision. Bioinformatics 36, i490–i498 (2020).
45. Weber, L. et al. PEDL+: protein-centered relation extraction from PubMed at your fingertip. Bioinformatics 39, btad603 (2023).
46. National Research Council (US) Committee. Recognition and Alleviation of Pain in Laboratory Animals. 12526 (National Academies Press, Washington, D.C., 2009). doi:10.17226/12526.
47. Wheat, N. J. & Cooper, D. M. A simple method for assessing analgesic requirements and efficacy in rodents. Lab Anim 38, 246–247 (2009).

48. Carbone, L. & Austin, J. Pain and Laboratory Animals: Publication Practices for Better Data Reproducibility and Better Animal Welfare. PLoS One 11, e0155001 (2016).
49. Jirkof, P. Side effects of pain and analgesia in animal experimentation. Lab Anim 46, 123–128 (2017).
50. Oh, S. S. & Narver, H. L. Mouse and Rat Anesthesia and Analgesia. Current Protocols 4, e995 (2024).
51. Jóźwiak-Bebenista, M. & Nowak, J. Z. Paracetamol: mechanism of action, applications and safety concern. Acta Pol Pharm 71, 11–23 (2014).
52. Potential anti-inflammatory role of paracetamol in knee OA. Nat Rev Rheumatol 3, 67–67 (2007).
53. Ayoub, S. S. Paracetamol (acetaminophen): A familiar drug with an unexplained mechanism of action. Temperature (Austin) 8, 351–371 (2021).
54. Boulares, A. H., Giardina, C., Inan, M. S., Khairallah, E. A. & Cohen, S. D. Acetaminophen inhibits NF-kappaB activation by interfering with the oxidant signal in murine Hepa 1-6 cells. Toxicol Sci 55, 370–375 (2000).
55. Posadas, I., Santos, P. & Ceña, V. Acetaminophen induces human neuroblastoma cell death through NFKB activation. PLoS One 7, e50160 (2012).
56. Saeed, I., La Caze, A., Hollmann, M. W., Shaw, P. N. & Parat, M.-O. New Insights on Tramadol and Immunomodulation. Curr Oncol Rep 23, 123 (2021).
57. RÖMPP Lexikon Chemie, 10. Auflage, 1996-1999: Band 2: Cm - G. (Thieme, Stuttgart, 2014).
58. Bianchi, M., Rossoni, G., Sacerdote, P. & Panerai, A. E. Effects of tramadol on experimental inflammation. Fundam Clin Pharmacol 13, 220–225 (1999).
59. Duthie, D. J. Remifentanil and tramadol. Br J Anaesth 81, 51–57 (1998).
60. Adelakun, S. A., Ukwenya, V. O. & Akintunde, O. W. Vitamin B12 ameliorate Tramadol-induced oxidative stress, endocrine imbalance, apoptosis and NO/iNOS/NF-κB expression in Sprague Dawley rats through regulatory mechanism in the pituitary-gonadal axis. Tissue Cell 74, 101697 (2022).
61. Rascol, O., Fabbri, M. & Poewe, W. Amantadine in the treatment of Parkinson's disease and other movement disorders. Lancet Neurol 20, 1048–1056 (2021).
62. Danysz, W., Dekundy, A., Scheschonka, A. & Riederer, P. Amantadine: reappraisal of the timeless diamond-target updates and novel therapeutic potentials. J Neural Transm (Vienna) 128, 127–169 (2021).
63. Pud, D. et al. The NMDA receptor antagonist amantadine reduces surgical neuropathic pain in cancer patients: a double blind, randomized, placebo controlled trial. Pain 75, 349–354 (1998).
64. Lascelles, B. D. X. et al. Amantadine in a multimodal analgesic regimen for alleviation of refractory osteoarthritis pain in dogs. J Vet Intern Med 22, 53–59 (2008).
65. Kubera, M. et al. Inhibitory effects of amantadine on the production of pro-inflammatory cytokines by stimulated in vitro human blood. Pharmacol Rep 61, 1105–1112 (2009).
66. Jiménez-Jiménez, F. J., Alonso-Navarro, H., García-Martín, E. & Agúndez, J. A. G. Anti-Inflammatory Effects of Amantadine and Memantine: Possible Therapeutics for the Treatment of Covid-19? J Pers Med 10, 217 (2020).
67. Hinrichs, M., Weyland, A. & Bantel, C. [Piritramide : A critical review]. Schmerz 31, 345–352 (2017).
68. Kay, B. A clinical investigation of piritramide in the treatment of postoperative pain. Br J Anaesth 43, 1167–1171 (1971).
69. Fischer, A. H., Jacobson, K. A., Rose, J. & Zeller, R. Hematoxylin and eosin staining of tissue and cell sections. CSH Protoc 2008, pdb.prot4986 (2008).
70. Chetty, R. & Gatter, K. CD3: Structure, function, and role of immunostaining in clinical

practice. The Journal of Pathology 173, 303–307 (1994).
71. Dos Anjos Cassado, A. F4/80 as a Major Macrophage Marker: The Case of the Peritoneum and Spleen. Results Probl Cell Differ 62, 161–179 (2017).
72. Uxa, S. et al. Ki-67 gene expression. Cell Death Differ 28, 3357–3370 (2021).
73. Yamashita, M. S. de A. & Melo, E. O. Mucin 2 (MUC2) promoter characterization: an overview. Cell Tissue Res 374, 455–463 (2018).
74. Erben, U. et al. A guide to histomorphological evaluation of intestinal inflammation in mouse models. Int J Clin Exp Pathol 7, 4557–4576 (2014).
75. Mann, E. R. et al. Compartment-specific immunity in the human gut: properties and functions of dendritic cells in the colon versus the ileum. Gut 65, 256–270 (2016).